NEGEM

Quantifying and Deploying Responsible Negative Emissions in Climate Resilient Pathways

Global assessment of NETP impacts utilising concepts of biosphere integrity

Horizon 2020, Grant Agreement no. 869192

Number of the Deliverable	Due date	Actual submission date
D3.3	**31.05.2023**	**31.05.2023**

Work Package (WP): 3 – Impact Assessment

Task: 3.1.2 Biosphere integrity: Biodiversity, nature conservation, vegetation properties

Lead beneficiary for this deliverable: PIK
Editors/Authors: Constanze Werner (PIK), Johanna Braun (PIK), Wolfgang Lucht (PIK), Dieter Gerten (PIK)

Dissemination level: Public

Call identifier: H2020-LC-CLA-02-2019 - Negative emissions and land-use based mitigation assessment

Document history

V	Date	Beneficiary	Author/Reviewer
1.0	2023-05-15	PIK	Constanze Werner; Johanna Braun; Wolfgang Lucht; Dieter Gerten/Lorie Hamelin, Kirsi Tiusanen
1.1	2023-05-30	PIK	Constanze Werner; Johanna Braun; Wolfgang Lucht; Dieter Gerten

NEGEM

Partners

VTT – VTT Technical Research Centre of Finland Ltd, Finland
PIK - Potsdam Institute for Climate Impact Research, Germany
ICL - Imperial College of Science Technology and Medicine, United Kingdom
UCAM - University of Cambridge, United Kingdom
ETH - Eidgenössische Technische Hochschule Zürich, Switzerland
BELLONA - Bellona Europa, Belgium
ETA - ETA Energia, Trasporti, Agricoltura, Italy
NIVA - Norwegian Institute for Water Research, Norway
RUG - University of Groningen, Netherlands
INSA - Institut National des Sciences Appliquées de Toulouse, France
CMW - Carbon Market Watch, Belgium
UOXF - University of Oxford, United Kingdom
SE - Stockholm Exergi, Sweden
St1 - St1 Oy, Finland
DRAX - Drax Power Limited, United Kingdom
SAPPI - Sappi Netherlands Services, The Netherlands

Executive Summary

As biosphere integrity is one of the main pillars of Earth system resilience along with climate stability, perspectives integrating climate and biosphere stewardship are urgently needed for indicating and navigating pathways that preserve a stable planet capable of providing sufficient life support for future generations on Earth. The deployment of negative emission technologies and practices (NETPs) requires careful consideration in the context of such pathways as the current climate economic analysis substantially entails both, a capacity to mitigate climate change by extracting CO_2 from the atmosphere and the potential to thereby further degrade biosphere integrity, especially when considering land use intensive NETPs. While earlier impact assessments have considered selected environmental effects of the deployment of biomass-based NETPs, their effect on biosphere integrity in its role for maintaining Earth system functioning has not yet been quantified in the context of NETP deployment using computable metrics.

This deliverable presents an assessment of the impacts of the two most land use intensive NETPs, plantation-based BECCS and reforestation, on functional biosphere integrity. It demonstrates in a quantitative manner and at the global scale that reforestation can add to climate stabilization while significantly contributing to the restoration of biosphere integrity, whereas BECCS may exacerbate the stress on biosphere integrity in an already severely strained system even when deployed on lands currently used as pastures. In terms of integrated climate stabilization and biosphere stewardship for the resilience of the entire Earth system, reforestation on pastures could thus be considered the preferable option, particularly for large-scale conversions and if extensive management on biomass plantations cannot be guaranteed globally. Along this message, the results provide quantifications for dynamics that have been described in a more qualitative matter before, as for example summarized in the IPCC's Special Report on Climate Change and Land in Chapter 6 (Smith et al., 2019).

For the analysis, we applied the dynamic global vegetation model LPJmL to simulate biogeochemical processes of the biosphere under different scenarios of expanding either biomass plantation or forest area, that informed two computable biosphere integrity metrics: (1) M-COL, assessing the impact of human colonization on the biosphere by estimating the amount of natural net primary production (NPP) – a proxy for the energy flow required to maintain planetary ecological functions – that is appropriated by humans and (2) M-ECO quantifying the deviation of an ecosystem from its pre-industrial (Holocene) state, in terms of vegetation structure, water fluxes, and carbon (C) and nitrogen pools and flows, i.e. quantifying biogeochemical disruption as a proxy for a more general risk of ecological disruption.

As the allocation of areas for NETPs may lead to trade-offs with conservation of remaining natural systems as well as global food security, the only viable option is a reduction in agricultural land without loss in calorie supply. This is in line with the findings of Deliverable 3.2 that any conversion of (semi-)natural land for BECCS would further undermine terrestrial planetary boundaries. Therefore, we focus on land allocation for NETPs within the bounds of current land use in this deliverable. Depending on the degrees to which a global transition to a healthier diet with less livestock products aligned with the EAT-Lancet planetary health diet is successful, pasture areas are converted to biomass plantations or reforestation in the scenarios assessed.

We find that the transition to the planetary health diet could substantially decrease the demand for grazing and release around 800 million hectares of pastureland, which could then be utilized for either reforestation or BECCS feedstock supply. If these areas were used for biomass plantations supplying BECCS, approximately 9–14 $GtCO_2eq$ yr^{-1} could potentially be removed depending on the BECCS technology applied (biomass-to-biofuel production or biomass-to-electricity). Such large-scale expansion of biomass plantations would however drastically reduce the energy available for the Earth system to maintain key biosphere functions by another

2.36 Gt C yr^{-1} on top of the already severe human appropriation of 11.26 Gt C yr^{-1}, as quantified by M-COL. Furthermore, it would increase the area that is subject to major or severe biogeochemical, hydrological and vegetation-structural shifts, evaluated by M-ECO, from 26% to 29% of the global land cover with the most affected biomes shifting even further away from the Holocene state than under current land use. As the alterations of flows, stocks, and vegetation structure of all affected biomes is found to become more pronounced under BECCS deployment, it is emphasized that plantation-based NETPs are challenging to align with internationally agreed-upon targets for nature restoration, like Goal A of the Kunming-Montreal Global biodiversity framework calling for the "integrity, connectivity and resilience of all ecosystems ... [to be] maintained, enhanced, or restored" (CBD, 2022) by 2050.

If the released pasture areas were reforested instead, less CO_2 would be removed per rededicated area compared to BECCS, with a simulated CDR of ~4.3 GtCO$_2$eq yr^{-1} for a full transition to the planetary health diet. Furthermore, reforestation bears inherent risks of CO_2 being released back into the atmosphere due to natural disturbances or anthropogenic factors. However, in terms of functional biosphere integrity, the analysis of M-COL found that reforestation provides an option to contribute to climate stabilization without further pressure on the availability of photosynthetically derived energy for the biosphere. In addition, the areas experiencing major shifts in key biospheric properties can be reduced from 18% to 16% and areas with severe shifts from 8% to 6%, which compares to half of the area affected severely in the BECCS scenario. The M-ECO evaluation further showed that reforestation can even significantly contribute to restoring key properties at biome scale by shifting elementary stocks, flows and structures back towards the natural state.

By enabling numerical assessments of biosphere integrity under different future scenarios, the metrics M-COL and M-ECO were found to qualify as tools to help identify and navigate development pathways that stabilize both the climate and biosphere as fundamental pillars of a functioning Earth system. The findings of this deliverable emphasize the need for a comprehensive approach to climate and biosphere stewardship, as we show that the type and extent of NETP deployment have significant implications for biosphere integrity, with BECCS imposing greater pressure and reforestation alleviating it. Therefore, the results highlight the importance of multi-dimensional assessments for NETP deployment in the EU and beyond, considering all aspects of Earth system stability as well as socioeconomic effects. Coordinated efforts of science and policy are, thus, required to develop strategies addressing the two intertwined crises of climate change and loss of biosphere integrity, while also integrating the urgently needed transformations of the food system. To achieve this, the global perspective presented in this report needs to be complemented by analyses that focus on the specific conditions within EU countries, as envisioned in the objectives of the NEGEM project.

Table of contents

List of figures

List of tables

1 Introduction

Biosphere integrity is one of the main pillars of Earth system resilience along with climate stability (Steffen et al., 2015). An intact biosphere regulates flows of energy, water, nutrients and materials and thus increases the Earth system's resilience to disturbances and disruptions (Aragão, 2012; Friedlingstein et al., 2022; Rockström et al., 2021; Sterling et al., 2013). However, human activity has become a major driver in the functioning of the biosphere, exerting a substantial impact on the Earth System, thereby posing a threat to the resilience of social and ecological systems (Folke et al., 2011). All biomes worldwide exhibit alarming reductions in areas not impacted by anthropogenic activities, with less than 1% of temperate grasslands, tropical coniferous forests, and tropical dry forests displaying very low human influence (Riggio et al., 2020). This occurs within the context of a global biodiversity crisis (IPBES, 2019), to which agriculture contributes most (Benton et al., 2021; Campbell et al., 2017), and the international appeal for enhanced protection and restoration of nature, as agreed upon in the recent Kunming-Montreal global biodiversity framework. As evidence of the biosphere's capacity to maintain Earth system stability continues to accumulate, it becomes increasingly imperative that preserving a stable planet capable of providing sufficient life support for future generations on Earth requires not only climate change mitigation but also biosphere stewardship (Rockström et al., 2021).

This perspective, integrating climate and biosphere stabilization, becomes particularly relevant when developing deployment pathways of negative emission technologies and practices (NETPs): On the one hand, NETPs extracting CO_2 from the atmosphere are being discussed as a key strategy for net emission reductions and fulfilling net zero emission targets, but on the other hand, they were also found to potentially induce further pressure on biosphere integrity (e.g. by land use expansion and intensification for biomass-based NETPs, (Humpenöder et al., 2018; Stenzel et al., 2021)). Although impact assessments have considered selected environmental effects of NETPs (Boysen et al., 2017; Heck et al., 2018; Humpenöder et al., 2018; Stenzel et al., 2021), the impact on functional biosphere integrity in its role of maintaining Earth system functioning has not yet been quantified in the context of NET deployment.

For example, Boysen et al. (2017) found substantial trade-offs between BECCS feedstock production and nature protection, which was reinforced by an assessment by Humpenöder et al. (2018) that additionally indicated significant nitrogen losses and water withdrawals for the large-scale establishment of biomass plantations. Extensive irrigation of these plantations could even expand the global area under water stress significantly, as found by Stenzel et al. (2021). These results are consistent with the findings by Heck et al. (2018) that allocating large areas for biomass plantations is difficult to reconcile with four terrestrial planetary boundaries (i.e. critical thresholds of anthropogenic interference with key Earth system processes): land use change, freshwater use, the biogeochemical flow of nitrogen and biosphere integrity. The latter was in this case estimated by the proxy of endemic species richness, thus focusing on the genetic component of biosphere integrity rather than the functional intactness (see below).

However, measuring the impacts of anthropogenic interference with biosphere integrity in its role of contributing to Earth system stability remains a major challenge. A decline in genetic biosphere integrity is a matter of extinction which requires scaling up local species censuses from diverse habitats to larger scales in order to draw conclusions about the biosphere. Exposito-Alonso et al. (2022) estimate that over the past 150 years, more than 10% of plant and animal species have become extinct, while IPBES (2019) estimates that another >10% of plant and animal species are currently threatened with extinction. Further pressures, i.e. by

large-scale NETP deployment, will depend on the specific exposure and vulnerability of individual species as well as intensity of the interference. Complementary to the genetic component representing the capacity of lifeforms to coevolve, persist and adapt under changing abiotic conditions, biosphere integrity can be assessed in terms of functional intactness supporting overall Earth system functioning (Steffen et al., 2015). Different approaches have been proposed to assess the interference of humans with functional biosphere integrity, including the assessment of the human footprint by Venter et al. (2016), based on remotely-sensed and bottom-up survey information, and the previously mentioned biosphere integrity indicator (BII) by Newbold (2018), integrating empirical site data and land cover maps.

The BII has been used to assess the effects of NETP deployment on biosphere integrity by considering critical thresholds in Deliverable 3.2 (Braun et al., 2022) and by evaluating a sustainable development pathway assessed in Soergel et al. (2021), leading to significantly lower BECCS potentials than the majority of IPCC scenarios compatible with a maximum warming of 1.5° or 2°C. However, the metric evaluates species abundance as a proxy for genetic integrity of the biosphere but is not explicitly associated with its functional integrity. Additionally, concerns have been raised about the explanatory value of the BII and its moderate response in substantially impacted regions (Martin et al. 2019). Hence, there is an urgent need for a robust assessment of the impacts of NETPs on the functional integrity of the biosphere, given that the potential scale of these interventions may significantly compromise this fundamental pillar of Earth system functioning.

Furthermore, the significance of indicators based on empirical data is restricted when it comes to future scenarios of global scale, such as the assessment of NETP deployment pathways. Computable metrics relying on process-based simulations, in contrast, offer the advantage that their explanatory power is not diminished when applied to future projections, where we encounter conditions that are often not represented in current empirical data, particularly not at a global scale.

One suitable candidate for such a metric is M-COL which is assessing the impact of human colonization on the biosphere by estimating the amount of natural net primary production (NPP) – the energy available to the natural biosphere to drive its multitude of ecological processes, from maintenance, growth and reproduction to building the exchanges essential to forming ecosystems – that is appropriated by humans. Based on the development by Stenzel et al. (2023), the metric is rooted in the HANPP (human appropriation of net primary production) framework (Haberl et al., 2007) and quantifies the amount of biomass extracted and the degree to which natural NPP is prevented by human activities. Extraction is accounted for as harvested carbon from cropland and biomass plantations as well as energy leaving grazing systems (i.e. while biomass that is consumed by ruminants may be returned to soils by excrements, we only account for the carbon losses in form of livestock respiration, products and livestock methane emissions). Additionally, the component of inhibited NPP involves comparing a scenario with human land use (e.g. pasture rededication to land-based NETPs) to a world without human land use, both under the same climate conditions.

Another metric that has been proposed for assessing key biosphere functions is M-ECO, also referred to as the Gamma Metric introduced by Heyder et al. (2011) and adapted by Ostberg et al. (2018) and Stenzel et al. (2023). It assesses the deviation of a system from a reference condition, for instance the Holocene state, in terms of vegetation structure, water fluxes, and carbon and nitrogen pools and flows. On a scale ranging from 0 (no alteration) to 1 (very significant alteration), elevated M-ECO values correspond to a higher risk of ecosystem destabilization, since more pronounced changes in biogeochemical, hydrological, or vegetation-structural features imply changes in the fundamental characteristics of the system, food chains, and species composition.

Addressing the pressing question of potential impacts of extensive land-based NETP deployment on biosphere integrity, this deliverable explores M-COL and M-ECO in regard to (i) their response to large-scale BECCS implementation and reforestation and (ii) the conclusions that can be drawn from the results regarding NETP impacts and the suitability of the metrics to assess these.

These aspects are assessed in a scenario framework developed in Deliverable 3.7 which involves allocating parts of current pasture area to BECCS or reforestation following assumptions of diet changes towards less livestock products. As the Deliverable 3.2 found that any conversion of (semi-)natural land for CDR would further undermine terrestrial planetary boundaries, land-based CDR would require a deep transformation of the food system to release land for climate stabilization within current land use bounds, if further biosphere degradation was to be avoided. In this regard, diet changes towards less livestock consumption hold promise as large areas could be reallocated from pasture areas without counteracting food security. In this context, the EAT-Lancet commission proposed a planetary health diet benefiting both food security and Earth system resilience, i.e. compliance with planetary boundaries. Emphasizing the consumption of plant-based products (including whole grains, fruits, vegetables, nuts and legumes), while reducing the intake of animal-based foods (particularly red and processed meat), a global transition to such a diet could serve human and environmental health (Springmann et al., 2016; Willett et al., 2019) thereby unlocking synergies with multiple SDGs (Chen et al., 2022).

By integrating a systematic analysis of functional biosphere integrity with this promising scheme that allocates pasture land to NETPs enabled by diet changes, Deliverable 3.3 aims to extend the analytical knowledge on sustainable NETP deployment pathways. This report therefore delves into several research questions:

- How can the impact of large-scale reforestation and establishment of biomass plantations for BECCS on the biosphere be quantified in an aggregate way?
- What are the impacts on functional biosphere integrity assuming pasture rededications to BECCS feedstock production or reforestation in line with a transition to the EAT Lancet planetary health diet?
- What conclusions can be drawn for the two computable metrics, when evaluating their values under NETP deployment?

In the assessment, the dynamic global vegetation model LPJmL (Schaphoff, von Bloh, et al., 2018; von Bloh et al., 2018) is applied to simulate spatially explicit responses of the coupled carbon, water and nitrogen cycles to pasture rededication. This enables the quantification of net CDR volumes based on process-based growth dynamics (see 2.1) along with the respective dynamically simulated impacts, for which we consider the transition of two land use intensive NETPs: the conversion to biomass plantations for BECCS with three different management scenarios (minimal, moderate, and intensive) and reforestation through assisted regrowth of natural vegetation to restore natural carbon pools. For the evaluation of the impact of these NETPs on functional biosphere integrity, we quantify the changes in key ecosystem processes in response to their deployment by M-COL and M-ECO as two computable metrics indicating shifts in functional biosphere integrity.

Deliverable 3.3 and Deliverable 3.7 can be considered as complementary and mutually reinforcing analyses. While this deliverable focuses on the NETP impacts on biosphere integrity and its measurability, Deliverable 3.7 evaluates the changes in demand for arable land, fertilizer and irrigation water as well as the impacts on water stress and three terrestrial planetary boundaries (nitrogen flows, freshwater change and land-system change) resulting from the pasture rededication scenarios. Certain sections of this report include (a summary of) the scenario development and results for CDR potentials covered in more detail in Deliverable 3.7, as indicated accordingly.

2 Methods

Following an overview of LPJmL as the modelling basis (see 2.1), we provide a description of the process involved to generate the scenarios for pasture rededication corresponding to the complete or partial adoption of the EAT-Lancet planetary health diet (see 2.2). Additionally, we outline the methodology employed to calculate net CDR potentials and the resulting impacts on functional biosphere integrity using the M-COL and M-ECO metrics (see 2.4).

2.1 LPJmL
[The contents of this section are identical to those of the corresponding section in the complementary Deliverable 3.7]

For the quantification of CDR potentials and environmental impacts, we apply the dynamic global vegetation model (DGVM) LPJmL, a well-established tool to assess climate and land use change impacts on the terrestrial biosphere, agricultural/biomass production, as well as the carbon (C), nitrogen (N) and water cycle (Schaphoff, von Bloh, et al., 2018; von Bloh et al., 2018). LPJmL represents biogeochemical processes of the biosphere at a daily time step and a spatial resolution of 0.5° x 0.5° in a process-based, spatially-explicit manner (Figure 1). In our analysis, we employed the LPJmL5-NEGEM version, which was prepared in subtask 3.1.1 as detailed in Deliverable 3.1 and further adapted for fertilization dynamics on biomass plantations for the assessments in Deliverable 3.2. Since the latter report, we have revised the parametrization of herbaceous biomass plantations to better reflect key aspects of plant physiology and nitrogen recovery (see S1 and Table S 1). Note that these model improvements and other crop calibration in LPJmL are based on current crop performance and do not represent new breeds, emerging farming technologies or precision agriculture. For further information on the representation of biogeochemical dynamics and their validation, please refer to Schaphoff, von Bloh, et al. (2018), Schaphoff, Forkel, et al. (2018) and von Bloh et al. (2018).

LPJmL simulates key ecosystem functions of vegetation through representing 11 natural plant functional types (PFTs, see Table S 2), 13 crop functional types (CFTs) including managed grassland, and three fast-growing second-generation energy crops. These bioenergy functional types (BFTs) are further categorized as herbaceous types (C4 grass) and woody types (eucalyptus, poplar, and willow based on the climate zone).

While the model simulates competition among natural plant functional types (PFTs) for light, water and nutrients, the distribution of crops and pasture is determined by a scenario-specific land use input that specifies the extent of irrigated versus rainfed areas. Irrigation water demand is internally computed for each cell and crop functional type (CFT) based on soil water deficit, with withdrawals from local renewable freshwater resources (river discharge, lakes and reservoirs) taking into account inefficiencies of prescribed irrigations systems (surface, sprinkler or drip irrigation) and constraints of local water availability after reductions through water withdrawals for households, industry and livestock (Jägermeyr et al., 2015). While the soil water deficit is dynamically modelled depending on daily climate input, soil type and crop species, the inefficiency of drip, sprinkler or surface irrigation systems is assumed to be fixed.

Carbon
GPP gross primary production
Ra autotrophic respiration
Rh heterotrophic respiration
Ch harvested carbon
Cf fire carbon fluxes
Csom soil organic matter C

Water
EI interception
ET transpiration
ES evaporation
P precipitation
perc percolation
infil infiltration
R runoff
Wreturn return flow of irrigation
Wirrig irrigation water
Q discharge

Energy
PAR photosynthetic active radiation
Rn net radiation

Nitrogen
BNF biological N fixation
Nf fertilizer/manure input
Nd atmospheric deposition
Nh harvested nitrogen
N_2 molecular N emission
N_2O nitrous oxide emissions
NH_3 ammonia volatilization
NO_x nitrogen oxides emissions
Nsom soil organic matter N
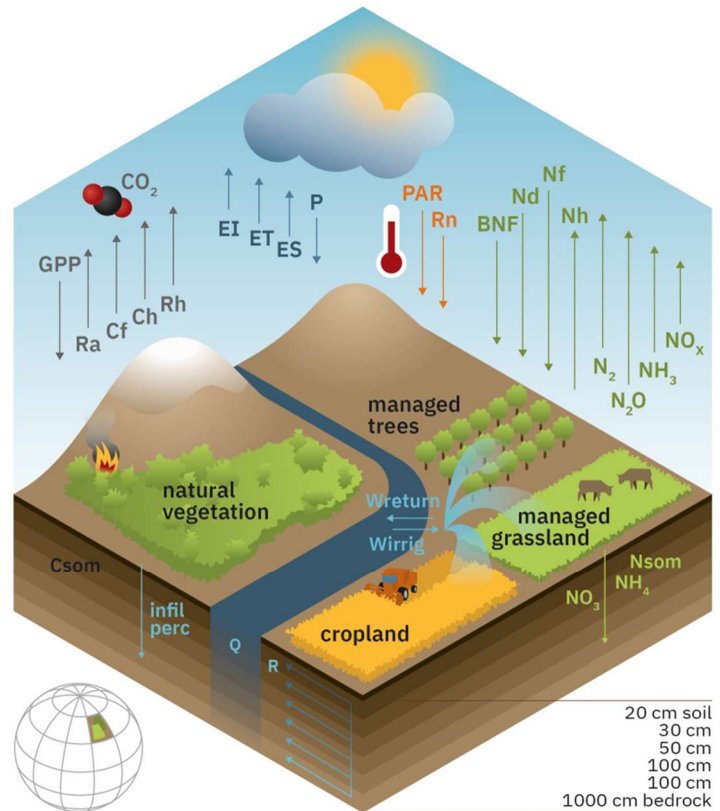
© LPJmL team

Figure 1 Schematic illustration of major processes represented in LPJmL.

LPJmL5-NEGEM further includes a representation of the nitrogen cycle that considers nitrogen-limited plant growth and ecosystem productivity by adjusting photosynthesis and respiration rates depending on the availability of nitrogen (von Bloh et al., 2018). The plant's uptake of nitrogen is determined by soil mineral nitrogen concentrations, soil properties, fine root mass, and plant demand for nitrogen. Inputs to the nitrogen pools in the soil (, NO_3^- and NH_4^+, and nitrogen of soil organic matter) are generated by decomposition of plant biomass, biological nitrogen fixation, atmospheric deposition and fertilization, the latter being prescribed by the input data for the scenario. By dynamically simulating the major flows of N, the model accounts for the mineralization of soil organic matter, immobilization, (de-)nitrification, and plant uptake within the nitrogen pools and represents losses to the atmosphere through (de-)nitrification or volatilization, as well as nitrate losses to renewable freshwater resources in runoff and leaching.

2.2 Scenarios
[This is a shortened version of the detailed description in the complementary Deliverable 3.7]

2.2.1 Pasture rededication scenarios

To estimate possible reductions in pasture extent in line with a global transition to the EAT Lancet planetary health diet, we first calculate the global proportion by which current grass feed could be reduced. Based on spatially explicit simulation of livestock densities and grazed biomass in LPJmL, we then rededicate current pasture areas to either biomass plantations or reforestation so that the rededicated areas correspond to the

calculated grazing reduction. This scenario design is shown in Figure 2 and described in more detail in Deliverable 3.7.

At the global level, the EAT Lancet diet implies a 70% reduction in ruminant meat consumption and an 8% increase in milk consumption in comparison to current consumption levels as reported by FAO for 2017 (FAO, 2023; Willett et al., 2019). Accounting for the different contributions of global grass feed to milk and meat production results in an overall reduction in grass feed by 46% (referring to dry matter) for a shift from current consumption patterns to the EAT Lancet diet. In addition to a scenario where the transition to the EAT Lancet diet is fully achieved (DC100), we also simulate scenarios with only partial transition to an EAT Lancet diet, i.e. where only half (DC50) or a quarter (DC25) of the grazing reduction is achieved.

We simulate rededication of current (2017) pasture extents corresponding to the calculated potential grazing reduction upon diet change. In this, we rely on the simulated spatially explicit grass feed uptake based on the livestock module implemented by Heinke et al. (2022) and calibrated to match the grazed biomass given in Herrero et al. (2013), as described in Deliverable 3.7. This enables to account for the fact that rededication of pastures with high grazing rates would result in stronger feed and thus animal product reductions than rededicating the same area within a minimally grazed rangeland. Thus, a grazing reduction by 46% must not equal a reduction in pasture area extent by the same proportion.
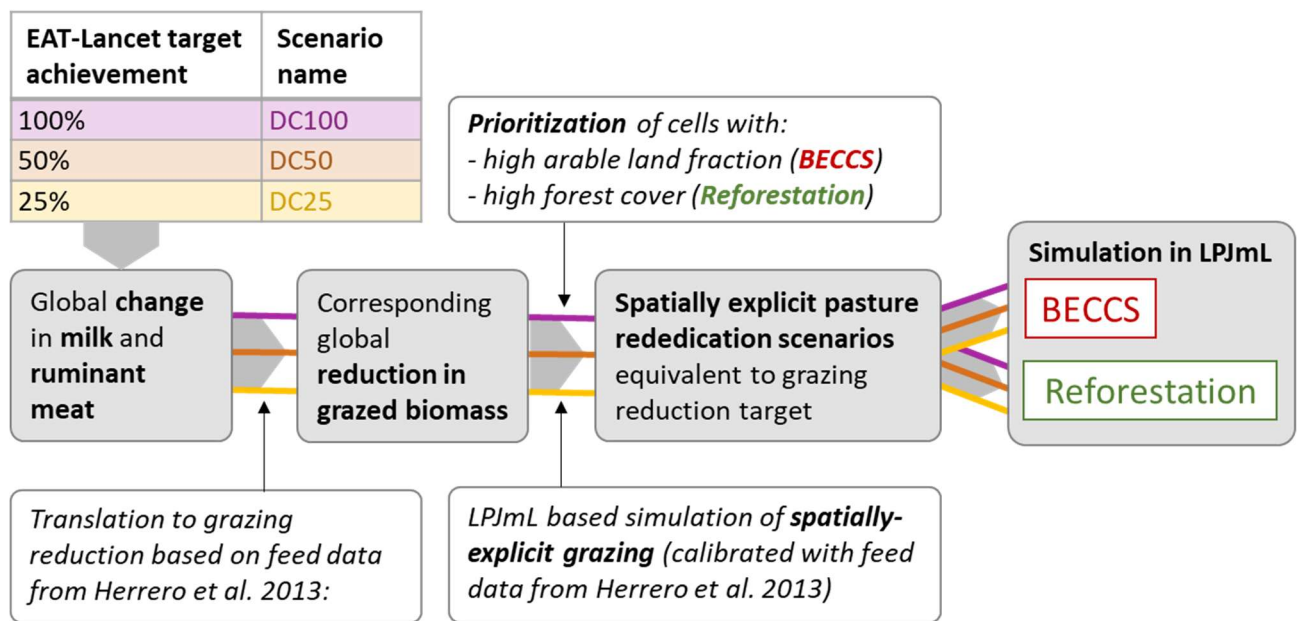
Figure 2. Overview on the approach to generate spatially-explicit scenarios of pasture conversion to either biomass plantations for BECCS or reforestation. For the description of the three BECCS management scenarios, see Table 1.

2.2.2   BECCS Scenarios

In the allocation scheme of biomass plantations for BECCS, we prioritize pasture areas in cells where we find the highest cropland fraction surrounding this land. This mirrors the high infrastructure needs for transport and processing of biomass for BECCS and the resulting economic advantages of building upon existing infrastructure. For the plantations, we assume herbaceous species because the current representation in LPJmL suggests that the herbaceous BFT has a considerable economic advantage over the woody type, owing to its higher yields and capacity for annual income generation. To capture the importance of water and nutrient management on plantations for both CDR and impacts, we developed three management scenarios spanning the range from

intensive to moderate and minimal management intensity, with cell-specific irrigation shares and nitrogen fertilizer application (see Table 1).

Table 1: Management scenarios for BECCS. CO_2 removal efficiency refers to losses along the BECCS supply chain (Deliverable 3.2) for either a biomass-to-electricity (B2E) or biomass-to-liquid pathway (B2L). N = Nitrogen. For a detailed description of the scenario assumptions, see Deliverable 3.7.

management scenario	irrigation	fertilization	CO_2 removal efficiency B2E	CO_2 removal efficiency B2L
intensive	irrigation share as for crops, but min. 30% of rededicated cell area	2 x N harvest under unlimited N conditions	0.923	0.669
moderate	irrigation share as for crops, but max. 30% of rededicated cell area	1 x N harvest under unlimited N conditions	0.836	0.603
minimal	rainfed	0	0.795	0.583

Net CDR from BECCS was calculated for each of the management and diet change scenarios by multiplying harvested carbon with a CO_2 removal efficiency along the BECCS supply chain and subtracting land use change emissions and additional nitrous oxide emissions – both dynamically simulated in LPJmL. Thus, we assess the main CO_2 streams along the supply chain plus N_2O emissions as an additional important contributor to climate effectiveness of the NETPs (see also Deliverables 3.2 and 7.3 (Chiquier, Patrizio, Sunny, et al., 2022)).

For the CO_2 removal efficiency, we assumed three scenarios for biomass to electricity (B2E) conversion (high, medium and low efficiency) from the MONET framework with a detailed representation of the BECCS supply chain (Chiquier, Patrizio, Bui, et al., 2022) and linked these to the plantation management scenarios (see Table 1 and Deliverable 3.2 for an overview on assumptions regarding CO_2 capture rates, transport distance and carbon footprint of electricity amongst others). As an alternative, we estimated the CO_2 removal potential for biomass to liquid (B2L) conversion with a significantly lower removal efficiency (Table 1) due to substantial CO_2 emission during combustion. This case was included as it might play an important role for providing renewable energy for the transport sector (Leblanc et al., 2022).

2.2.3   Reforestation scenarios

Given the importance of intact forest landscapes for conservation (Betts et al., 2017), we prioritize reforestation on pastures in regions with high share of remaining forest cover. Due to reductions in albedo upon reforestation (e.g. Bonan, 2008; Pongratz et al., 2011; Sonntag et al., 2016) in the boreal zone and a resulting net warming effect, the described procedure only targets pastures in the temperate and tropical zone, but excludes reforestation in the boreal zone.

As we deliberately defined reforestation as the restoration of natural forest ecosystems (i.e. assuming native species and excluding harvesting, fertilization and irrigation), natural vegetation was simulated to regrow on reforested areas, undergoing establishment and competition among plant functional types as implemented in a process-based manner within LPJmL. This represents a practice of "abandoning" pastures and leave it to undergo natural processes without human intervention. Due to the absence of an explicit reforestation module, LPJmL cannot represent planted tree saplings of a pre-defined functional type and higher age. Instead the model simulates the competition of various plant types leading to a slower establishment and thus limited carbon accumulation within the first decades. Further improvement is required to enhance the delayed establishment, even when considering the approach of natural forest regrowth. A comparison to literature on aboveground

carbon accumulation rates in young natural forests (Cook-Patton et al., 2020) showed that the respective simulated rate is underestimated by a factor of ~2. We therefore assume that carbon pools after 60 years of simulation are reached within 30 years, and show that the thereby implied aboveground carbon accumulation rates match well both modelled rates in Cook-Patton et al. (2020) and 2019 IPCC defaults (IPCC, 2019) across biomes and continents (see Figure S 1). Furthermore, the simulations closely align with the observations collected by Cook-Patton et al. (2020) regarding the biome-specific median increment of carbon found on former pasture (see Figure S 2).

To simulate CDR potentials from reforestation, we compared carbon pools in vegetation, litter and soil between the scenario with reforestation on pastures in line with a diet change target and the agricultural reference of the year 2017 with unchanged land use patterns (see Figure 3). While natural fire disturbances are simulated in LPJmL, additional disturbances, such as pests or extreme weather events, and their impacts on sequestered carbon have not been accounted for.

2.3   Simulation setup
[The contents of this section are identical to those of the corresponding section in the complementary Deliverable 3.7]

All simulations of pasture rededication to biomass plantations for BECCS or reforestation were preceded by a 10,000-year spin-up of potential natural vegetation with 1901-1930 climate (input combining GSWP3 data with a bias-adjusted version of ERA5, Lange (2019)) to bring vegetation distribution and related carbon and nitrogen pools into equilibrium (see Figure 3). This was followed by a transient simulation of historical land use change from 1500 to 2017, with prescribed land use patterns as well as fertilizer and manure rates from Ostberg et al. (2023).
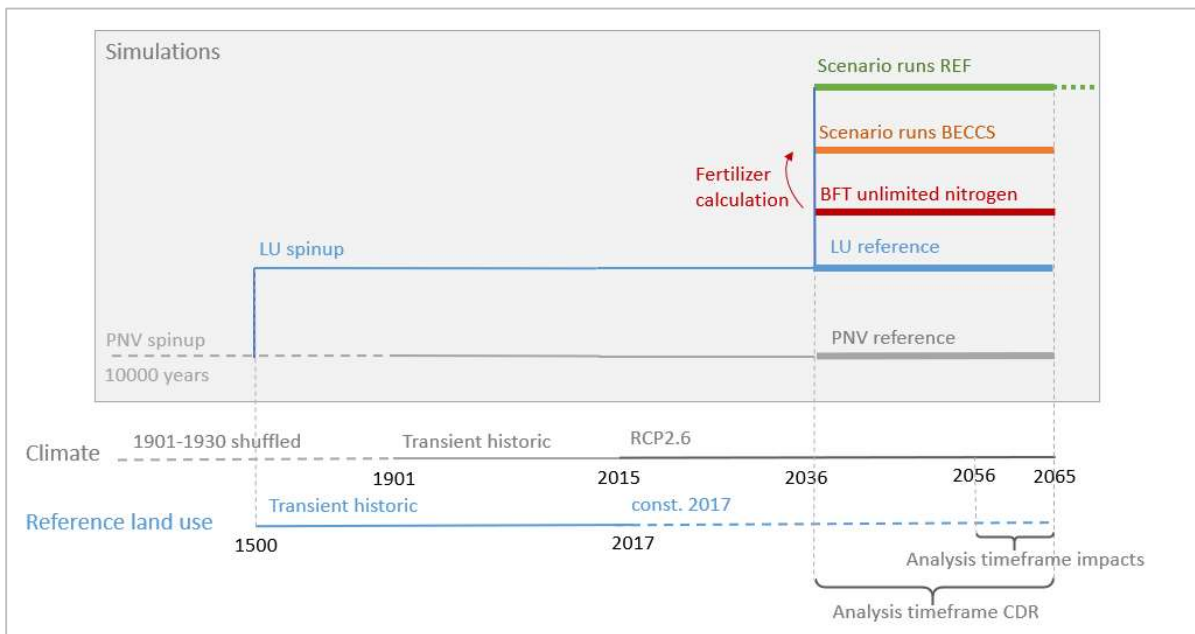
Figure 3: LPJmL simulation protocol. PNV = potential natural vegetation; LU = land use; BFT = bioenergy functional type (here: for representation of Miscanthus).

For simulations of mid-century CDR potentials from rededicated pastures to either biomass plantations for BECCS or reforestation, we adapted the 2017 land use pattern according to the scenarios (see above) and kept this pattern constant for 2036-2065 climate. As a reference for calculation of CDR and impacts, we simulated, for the same timeframe and climate, the counterfactual case of keeping 2017 land use constant over time (LU reference,

see Figure 3) and potential natural vegetation (PNV reference, no human land allocation globally, see Figure 3), amongst others for simulation of natural biome extents, incl. forest areas. Future climate inputs are based on a bias-correct version of data from the GFDL-ESM4 model for RCP2.6-SSP2 prepared by Lange and Büchner (2021), assuming climate change mitigation compatible with the Paris Agreement. While yearly CDR is averaged over a 30-year mid-century timeframe, the impacts of pasture rededication were calculated for the last 10 years of the respective analysis timeframe to better account for the committed impacts, which may be less pronounced in the first years after conversion. For calculation of CDR for reforestation, the simulation was extended by 30 years for a better match with literature on carbon sequestration rates.

2.4   Biosphere integrity metrics

The impacts on functional biosphere integrity are assessed for each BECCS and reforestation scenario by quantifying M-COL and M-ECO based on biogeochemical and vegetation-structural variables simulated by LPJmL. The following sections describe the composition and computation of these metrics. An R package incorporating the functions for calculating the metrics based on gridded input data will be made available with the publication of Stenzel et al. (2023).

2.4.1   M-COL metric

M-COL measures the impact of human colonization on the biosphere by estimating the extraction of biomass as well as the amount of natural net primary production (NPP) - the energy flow required to maintain planetary ecological functions - that is prevented through human interaction with the biosphere (e.g. through deforestation). The applied computation scheme for M-COL was developed by Stenzel et al. (2023) and is based on the HANPP framework by Haberl et al. (2007). However, unlike Haberl et al., who relied on inventory data for estimating biomass harvests and inhibited NPP, the novel approach employs dynamically simulated carbon flows provided by LPJmL outputs. This allows for spatially explicit and globally aggregated assessments as well as computation of M-COL based on historic patterns and future scenarios.

M-COL represents the combined value of intentionally extracted biomass ($NPP_{Harvest}$), which is evaluated as harvests and other removals on cropland, pastures and biomass plantations (in terms of NPP), along with the suppressed natural biomass production resulting from human land use changes ($NPP_{Land\ Use}$):

$$M\text{-}COL_{abs} = NPP_{Harvest} + NPP_{Land\ Use} \qquad (1)$$

Both components are regarded as photosynthetically derived energy that is no longer available for the biosphere. $NPP_{Harvest}$ comprises the harvest of crops and residues on arable land (including the harvest on biomass plantations) as well as carbon leaving grazing systems. As biomass that is consumed by ruminants may be returned to soils by excrements, we only account for the carbon losses in form of CO_2 emissions from livestock respiration, products and methane emissions. In LPJmL, pasture currently only represents ruminants as the major part of direct grazing, whereas fodder production for all animal husbandry is included as a crop functional type. Extractions from managed forests and biomass losses due to human induced fires can currently not be accounted for within process-based LPJmL simulations. $NPP_{Land\ Use}$ is derived by calculating the differencebetween the actual biomass production (NPP_{act}) of the assessed land use (e.g. current land use or future scenarios) and a scenario of potential natural vegetation without human land use under the same climate conditions (NPP_{pot}):

$$NPP_{Land\ Use} = NPP_{pot} - NPP_{act} \qquad (2)$$

If management increases the NPP compared to the potential natural vegetation, $NPP_{Land\ Use}$ may become negative. But this would only result in a decrease in M-COL, if the additional biomass was not extracted (i.e. $NPP_{Harvest}$ staying constant).
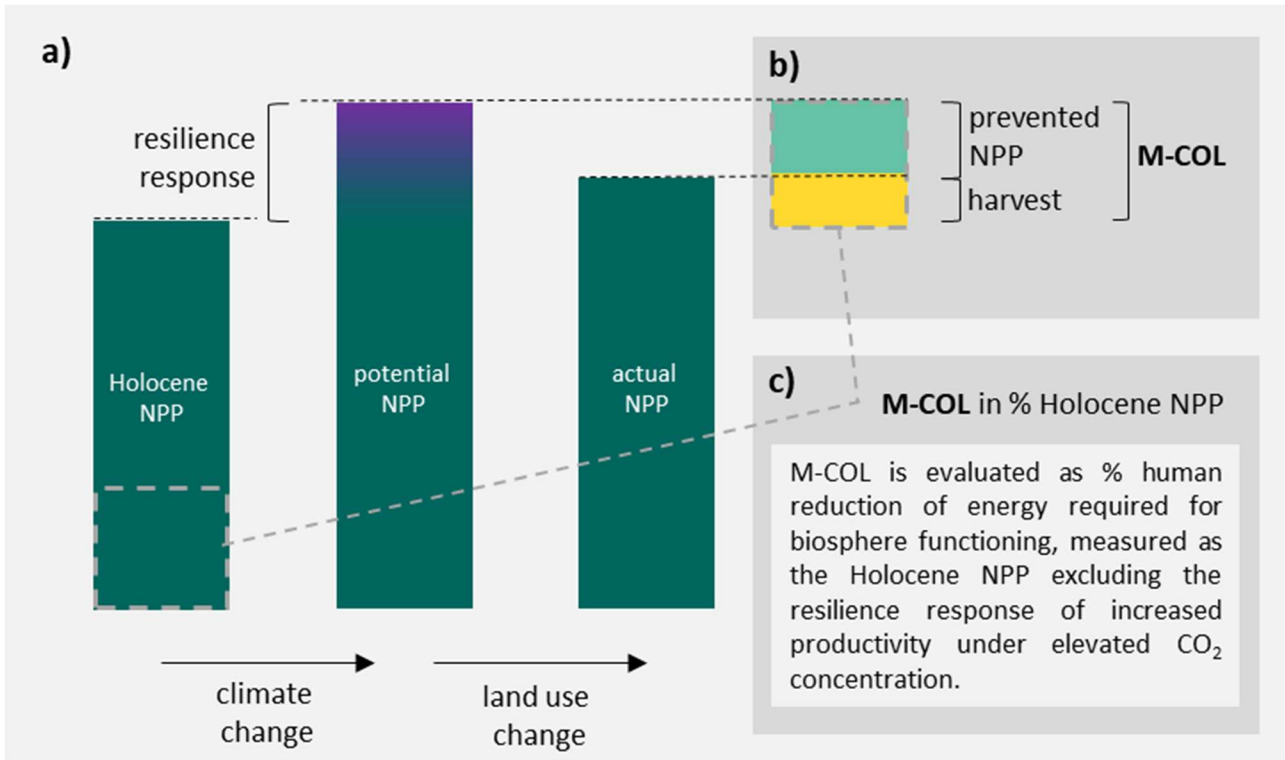
Figure 4. Schematic representation of the M-COL metric, including a) the net primary production (NPP) components considered with the actual NPP (e.g. current land use or future scenario) and potential NPP showing the potential NPP under changed climate but without human land use including an increase compared to the Holocene NPP, because the system is responding to the increased CO_2 in the atmosphere , b) the M-COLcomponents, prevented NPP (turquois) and harvest (yellow) and c) the evaluation reference.

The absolute value of M-COL ($M\text{-}COL_{abs}$) is further translated into a relative comparison to the Holocene NPP ($M\text{-}COL_\%$) to indicate the degree to which the photosynthetically-derived energy required to drive key ecological functions in a pristine Holocene biosphere has been appropriated by humans:

$$M\text{-}COL_\% = M\text{-}COL_{abs}/NPP_{Hol} \qquad (3)$$

Therefore, the NPP increase due to CO_2 fertilization caused by anthropogenic emissions is regarded as the resilience response of the biosphere to changing atmosphere and climate and cannot be used to compensate losses of biomass due to human land use or extraction. In this quantification, the NPP of the Holocene state (NPP_{Hol}) is simulated as potential natural vegetation under pre-industrial climate conditions of 1901-1930 (see Figure 3).

2.4.2 M-ECO metric

M-ECO assesses multidimensional changes in key biospheric characteristics as a representation of complex ecological transformations resulting from human interactions with the biosphere, e.g. deployment of land use intensive NETPs. This approach utilizes a proxy methodology based on the understanding that significant alterations in fundamental elements, such as carbon, nitrogen and water exchanges with the atmosphere and soil, or shifts in vegetation types and functional strategies, have implications for more intricate ecological structures, such as predator-prey and host-parasite relationships, competition and complementarity in resource utilization, and mutual interactions like pollination, which are challenging to model comprehensively at the global scale (Ostberg et al., 2013). These shifts in major ecological stocks, flows and structure are quantified by

comparing the state of the biosphere between the land use scenario of interest (i.e. current pattern, expansion of biomass plantations or reforestation) to a world without human land use under the same climatic conditions (see PNV reference in Figure 3) applying the computation scheme developed by Stenzel et al. (2023) based on Ostberg et al. (2018).

M-ECO is determined by combining four subcomponents: vegetation structure (vs), local change (lc), global importance (gi), and ecosystem balance (eb). Each of these subcomponents is measured on a scale of 0 to 1 (V, l, g, e) and then weighted by their corresponding change to variability ratio ($S(x, \sigma_x)$). To arrive at a composite score, the resulting values are finally averaged to compute the M-ECO metric:

$$M\text{-}ECO = \frac{vs + lc + gi + eb}{4} = \frac{V * S(V, \sigma_V) + l * S(l, \sigma_l) + g * S(g, \sigma_g) + e * S(e, \sigma_e)}{4} \qquad (4)$$

The change in vegetation structure (V) is derived by comparing the ecosystem states i and j (e.g. the land use scenario of interest and a PNV reference) in terms of the total ground cover area (A) of the specific ground cover type k, which includes tree, grass, and barren. These changes are further analysed by considering the differences in the area covered by each PFT (p) considering the attributes (l) that defines evergreenness, needleleavedness, tropicalness, borealness, and naturalness (refer to Table S 2 for more details on the specific attributes for each PFT).

$$V(i,j) = 1 - \sum_k \left\{ \min(G_{ik}, G_{jk}) * \left[1 - \sum_l \left(\omega_{kl} \left| \sum_p (A_{iklp} * a_{klp}) - \sum_p (A_{jklp} * a_{klp}) \right| \right) \right] \right\} \qquad (5)$$

Table 2. Processes and associated variable aggregation from LPJmL outputs.

Process description	LPJmL variable(s)
surface area covered by respective plant groups	Natural vegetation and bioenergy: foliage projected cover Crops: land use fraction
vegetation carbon pool	vegetation carbon
soil carbon pool	soil carbon + litter carbon
carbon losses into air	fire carbon emissions
carbon fixation	NPP
carbon losses	heterotrophic respiration + harvested carbon
vegetation nitrogen pool	vegetation nitrogen
soil nitrogen pool	soil NH_4^+ + soil NO_3^-
nitrogen losses into air	nitrogen volatilization + N_2 emissions + N_2O emissions from denitrification + nitrification
nitrogen fixation	biological nitrogen fixation
nitrogen losses into water	nitrogen leaching in runoff to surface water
productive evaporative water losses	transpiration
unproductive evaporative water losses	evaporation + interception
freshwater production	runoff
soil water content	soil water pool

The components l, g, and e are calculated by comparing two ecosystem state vectors, $\vec{s}_1$ (PNV reference) and $\vec{s}_2$ (state under human land use), comprised of biogeochemical variables $\vec{v}_{1,i}$ and $\vec{v}_{2,i}$, with $i = [1, ..., n]$ (see Table 2 for variables):

$$\vec{s}_1 = \begin{pmatrix} v_{1,1} \\ \vdots \\ v_{n,1} \end{pmatrix}, \vec{s}_2 = \begin{pmatrix} v_{1,2} \\ \vdots \\ v_{n,2} \end{pmatrix} \quad (6)$$

Local change (l) refers to the magnitude of differences in biogeochemical properties compared to the PNV reference, indicating the extent of local condition changes. This is calculated by normalizing the state variables with the corresponding values from the reference state:

$$\vec{s}_{l_1} = \begin{pmatrix} 1 \\ \vdots \\ 1 \end{pmatrix}, \vec{s}_{l_2} = \begin{pmatrix} v_{1,l} \\ \vdots \\ v_{n,l} \end{pmatrix} \quad (7)$$

$with\ v_{i,l} = \frac{v_{i,2}}{v_{i,1}}, for\ v_{i,1} \neq 0$

Global importance (g) contextualizes these local changes by comparing them to the global mean reference state. This approach recognizes that even minor changes on the local level may have significant impacts on larger scales if they are of a sufficient magnitude. To account for this, the state vectors of a given time ($v_{i,t}$) are normalized with the globally averaged reference mean value $\overline{v_{i,ref\ g}}$:

$$\vec{s}_{g_1} = \begin{pmatrix} v_{1,g,1} \\ \vdots \\ v_{n,g,1} \end{pmatrix}, \vec{s}_{g_2} = \begin{pmatrix} v_{1,g,2} \\ \vdots \\ v_{n,g,2} \end{pmatrix} \quad (8)$$

$$for\ \ v_{i,g,t} = \frac{v_{i,t}}{v_{i,ref\ g}}, for\ \overline{v_{i,ref\ g}} = \frac{1}{\sum a_p} \sum_{p=1}^{z} a_p v_{i,p} \neq 0$$

$$for\ cells\ p = 1, ..., z\ with\ cell\ area\ a_p$$

For local change and global importance, the difference between the two states is determined by the length of the difference vector between them:

$$d_l = \left| \overrightarrow{s_{l_2}} - \overrightarrow{s_{l_1}} \right| \ \ and\ \ d_g = \left| \overrightarrow{s_{g_2}} - \overrightarrow{s_{g_1}} \right| \quad (9)$$

And the values of the corresponding metric components l and g are computed by scaling d_l and d_g to a range between 0 and 1 applying the following sigmoid transformation function ($T(x)$):

$$l = T(d_l), g = T(d_g) \quad (10)$$

$$T(x) = A + \frac{1 - A}{1 + e^{-6(x - 0.5)}}, \ \ with\ A = -\frac{1}{e^3} \quad (11)$$

Ecosystem balance (e) measures changes in the relative importance of shifting biogeochemical properties in relation to one another, i.e. if a variable change is significantly more pronounced than others. This serves as an indicator for qualitative changes in the balance of dynamic processes that may indicate a disruption in ecological functioning (Ostberg et al., 2018).

The calculation is based on the angle α between the two state vectors, with normalization applied as done for local change:

$$b' = 1 - \cos(\alpha) = 1 - \frac{\vec{s}_{l_1} * \vec{s}_{l_2}}{|\vec{s}_{l_1}||\vec{s}_{l_2}|} \quad (12)$$

b' is scaled to a range from 0 and 1, with a value of 1 if the angle between the vectors >60°:

$$e = \begin{cases} b' * 2 & if\ \alpha \leq 60° \\ 1 & otherwise \end{cases} \quad (13)$$

Finally, the metric accounts for the interannual variability in the reference state to which ecosystems have adapted, recognizing that exceeding this magnitude of variability may render an ecosystem more vulnerable. This is done by weighting the four change components of the metric (V, l, g, e) with their corresponding change to variability ratio ($S(x, \sigma_x)$), see above. It is calculated based on the standard deviation (σx) of the corresponding component in the PNV reference:

$$S(x, \sigma_x) = \frac{1}{1 + e^{-4\left(\frac{x}{\sigma_x} - 2\right)}} \quad (14)$$

$$with\ \sigma_x\ as\ the\ interannual\ standard\ deviation\ of\ x\ under\ reference\ conditions$$

We calculate M-ECO for the current land use pattern as well as for the BECCS and reforestation scenarios (see 2.2) in relation to a counterfactual state with no human land use. This allows us to quantify the impact of current practices on essential ecological properties and to assess, moreover, the extent to which this impact can be amplified or mitigated through large-scale deployment of NETPs. While M-ECO is calculated at spatial resolution of LPJmL (0.5° x 0.5°), we also aggregate values to the biome and global level to serve the evaluation context of the global biosphere.

Furthermore, we evaluate the M-ECO values in terms of the global extent of three classes indicating moderate, major and severe shifts in biogeochemical and vegetation-structural properties of the biosphere. Similar to the approach by Ostberg et al. (2018), we classify M-ECO values >0.3 and <0.6 as major shifts, grounding on the difference between similar, yet distinct biomes, i.e. representing a transition from tropical rainforest to tropical deciduous forest (0.37) or warm grassland to temperate grassland (0.32). M-ECO values >0.6 are regarded as severe shifts that are stronger than the difference between significantly distinct biomes, i.e. warm woodland to tropical rainforest (0.59) or from temperate coniferous forest to tropical deciduous forest (0.56). An in-depth discussion of critical thresholds is provided in Stenzel et al. (2023).

3 Results

3.1 Net CDR potentials from rededicating pastures

[The contents of this section are identical to those of the corresponding section in the complementary Deliverable 3.7]

A full or partial transition to the EAT-Lancet planetary health diet could allow for conversion of 194, 388 and 836 Mha of pastures to biomass plantations for the DC25, DC50 and DC100 scenario, respectively, or alternatively for reforestation on 161, 325, and 736 Mha of pasture, at the global level (see Figure 5). This corresponds to rededication of ~5% (DC25) to ~25% (DC100) of global pasture areas (in year 2017), and compares to ~10% (DC25) to 50% (DC100) of global croplands (in year 2017). While the

EAT Lancet planetary health diet was calculated to imply a reduction in grazed biomass of 46%, pasture areas decrease only roughly half as much, as areas with above-average grazing intensities were selected for rededication in both allocation schemes. For biomass plantations, cells with a high share of arable land were prioritized (for economic and infrastructure reasons; see methods). This leads to rededicated pastures in regions with already intensive agriculture and mostly high population density first (see yellow areas in Figure 6a), further expanding into less intensively used areas in the higher pasture rededication scenarios. In contrast, reforestation starts in regions with highest remaining forest cover (for restoration of intact forest landscapes; see methods), thus expanding from pristine areas amongst others in the (sub-) tropics and mostly sparsely populated regions to areas with higher historical deforestation rates (see Figure 6a). These different allocation schemes also explain why the assigned global areas differ for biomass plantations and reforestation.
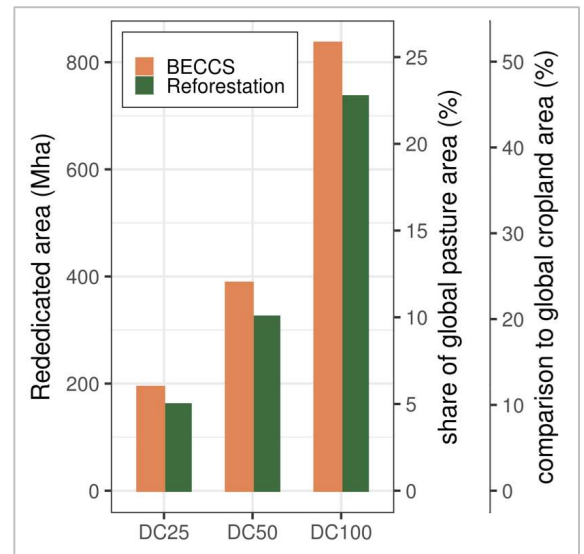

Figure 5: Global pasture areas rededicated to biomass plantations for BECCS or, alternatively, to reforestation in line with partial or full transition to an EAT-Lancet planetary health diet. Right axes show (i) the rededicated pasture area share and for contextualization (ii) the share of global cropland the areas would correspond to.

For BECCS with moderate management, simulated net CDR per area on rededicated pastures is highest in eastern China and US, as well as tropical Southeast Asia, where high precipitation levels boost productivity on rainfed plantations (see Figure 6b; for simulated net CDR in the minimal and optimal management scenarios see Figure S 4). Depending on the management and diet change scenarios, 12-25% of the originally harvested CO_2eq on biomass plantations are offset through land use change emissions (i), and 4-15% through additional N_2O emissions from fertilization (ii). Additional supply chain losses through fossil fuel use and the carbon capture and storage process (iii) range between 8 and 21% of the originally harvested CO_2eq for a more efficient B2E pathway and 33-42% for a B2L pathway, resulting in overall CO_2 removal efficiencies between 48-66% for B2E and 27-43% for B2L (see Figure S 5 for detailed breakdowns of net CDR calculation for all scenarios). Despite these inefficiencies, net CDR rates from biomass plantations for BECCS are generally higher as compared to respective CDR potentials from reforestation. For reforestation, pasture conversion is simulated to not always lead to net CDR both in temperate and tropical biomes (see red cells in Figure 6b), implying that aggregate soil, litter and vegetation carbon pools decrease as compared to pastures. It has been shown that pastures can have particularly high soil carbon pools with ~90% of sequestered carbon stored belowground and that light grazing, in contrast to heavy grazing, may increase soil organic carbon (Bai & Cotrufo, 2022). A transition from pastures to woody vegetation may lead to decreases in the accumulated soil carbon pools, at least within the first decades after tree establishment when growth in aboveground biomass may not compensate for potential losses in soil carbon (Conant et al., 2001; Cook et al., 2014; Friggens et al., 2020; Kirschbaum et al., 2008; Shen et al., 2023). Nevertheless, this model

behavior needs further investigation and testing, as site studies generally report overall increases in carbon stocks through forest regrowth on former managed grasslands, or (the other way round, forest conversion to pastures generally represents a loss in overall carbon pools (Conant et al., 2001; de Koning et al., 2003; Fearnside & Imbrozio Barbosa, 1998; Shen et al., 2023; Silver et al., 2004). Recovery of soil carbon accumulation rates and vegetation carbon built-up after reforestation might thus take too long in LPJmL.
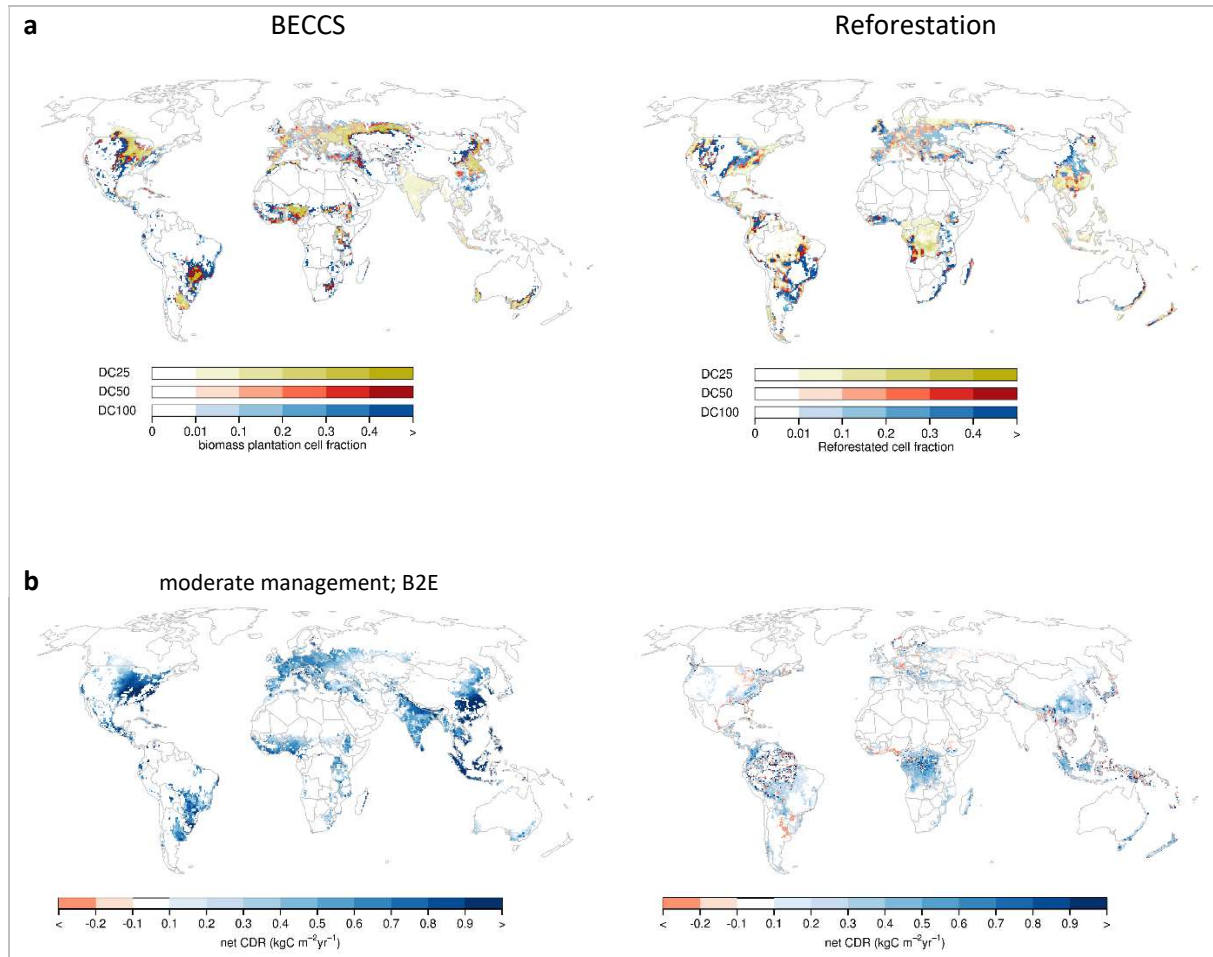

Figure 6: Simulated scenarios of rededicating pastures to biomass plantations for BECCS (left) or reforestation (right) in line with diet changes. (a) Geographic distribution of rededicated cell fractions corresponding to a 25% (yellow), 50% (red) and 100% (blue) transition to the EAT-Lancet planetary health diet. (b) Simulated net CDR per area for all cells with rededicated pastures in the 100% scenario. For BECCS, this refers to the moderate management scenario and biomass-to-electricity conversion (B2E; see methods). Negative net CDR (= net CO_2 emissions instead of removal) are displayed in red.

At the global level, a partial or full transition to the planetary health diet and associated reductions in pasture requirements could allow for the realization of high levels of CDR from BECCS or reforestation within current land use bounds. Establishment of biomass plantations on ~200Mha of pasture areas in line with a partial transition to the planetary health diet (DC25) may provide 3.3 GtCO$_2$eq yr^{-1} in the moderate management scenario (1.7 – 4.4 for minimal and optimal management) for the more efficient B2E pathway, and 2.0 Gt CO$_2$eq yr^{-1} (1.0 – 2.8) for a B2L pathway (see Figure 7a). For a full diet transition, this potential may be increased to up to 14.4 GtCO$_2$eq yr^{-1} (9.7 – 18.5) for B2E and 8.9 GtCO$_2$eq yr^{-1} (5.9 – 11.3) for B2L. Compared to CDR levels simulated in economically optimized climate mitigation scenarios included in the 6th Assessment Report of the IPCC (IPCC, 2022), the DC25 scenario is broadly in line with median BECCS rates in 2050, whereas the more comprehensive diet change scenarios better align with AR6 rates in 2100 (see Figure 7b). Note that this

comparison serves contextualizing purposes only, as (i) the Integrated Assessment Models (IAMs) covered in AR6 do not only assume biomass sources from additional dedicated biomass plantations and partly include additional feedstocks from agricultural and forestry residues as well as logs from managed forests (Hanssen et al., 2020; Rose et al., 2022) and (ii) the here presented scenarios assume large-scale and comprehensive diet shifts towards less livestock products, in contrast to most IAM scenarios.

For reforestation, the global numbers are generally lower than for BECCS, but in the lower scenarios still within the range of the B2L BECCS pathway (see Figure 7a). A full transition to the EAT-Lancet diet may allow for removal of up to ~4.3 GtCO$_2$eq yr^{-1} on reforested pastures, or 1.6 and 2.7 GtCO$_2$eq yr^{-1} for the DC25 and DC50 scenario, respectively. While net removal from managed land (integrating re-/afforestation and deforestation amongst others) in 1.5°-2°-compatible AR6 scenarios span a wide range, median net CDR in 2050 is comparable to the rates simulated in the DC50 scenario, while the most ambitious DC100 scenario is broadly in line with median AR6 rates in 2100 (Figure 7b). Land sparing and net reforestation in AR6 scenarios may however not only result from diet changes but also from productivity increases amongst others. Also, simulated reforestation rates may be underestimated due to too slow tree establishment and soil carbon loss in some cells (see above and discussion). Yet, exclusion of cells with net emissions upon reforestation only leads to a minor CDR increase by 0.5 GtCO$_2$eq yr^{-1} to 4.8 GtCO$_2$eq yr^{-1} in the DC100 scenario.
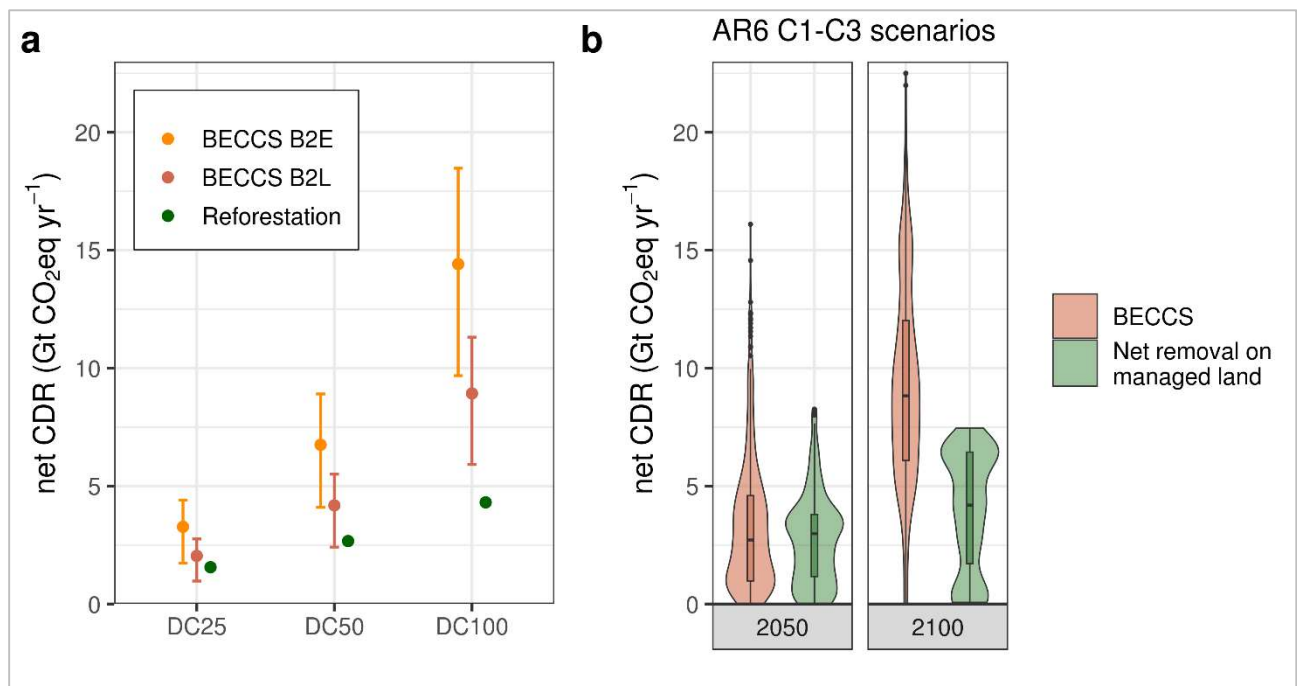
Figure 7: Global net CDR potential for BECCS and reforestation on pasture areas in line with full or partial transition to a planetary health diet (a). For BECCS, CDR rates for both a biomass-to-electricity pathway (B2E) and a biomass-to-liquid (B2L) pathway are displayed, referring to the moderate management scenario. Error bars delineate the range spanned by the minimal and intensive management scenarios. In (b) projected CDR rates for BECCS and managed land (net; integrating deforestation and re-/afforestation) from 1.5°-2°-compatible scenarios (categories C1-C3) included in the IPCC AR6 report (IPCC, 2022) are displayed for contextualization. Boxplots show medians and interquartile ranges, and kernel probability density of projected CDR rates is additionally displayed.

3.2   M-COL evaluations of biosphere integrity

When assessing the impact of NETP implementation on the availability of photosynthetically derived energy for the biosphere using M-COL, it is crucial to acknowledge the existing high level of stress on this system caused by human activities. Throughout history, the human appropriation of energy necessary to sustain biosphere functioning has evolved to a critical point. Today, the human land use has reached an appropriation of 11.26 Gt C yr^{-1}, which accounts for 17.25% of the Holocene NPP, and thus impairs the natural functioning of the biosphere (Figure 8a).

In the DC100 scenario, BECCS leads to an additional appropriation of 2.36–2.92 Gt C yr^{-1} compared to the land use reference. As a result, the proportion of the Holocene-NPP that is inaccessible for biosphere functioning increases to 21.27-22.11%, varying from intensive to minimal management (1.07-1.39 Gt C yr^{-1} and 19.29-19.79% for DC50, or 0.48-0.68 Gt C yr^{-1} or 18.40-18.70% for DC25, respectively, as shown in Figure 8). This transition under DC100 represents a shift in M-COL that corresponds to the changes observed over the last 50 years of human land use and intensification – yet, induced by BECCS feedstock production alone. For DC50 the difference compares to the shift over the last 20 years and for DC25 over the last decade. Due to the already significant loss of energy required for biosphere functioning resulting from human activities, any further acquisition of NPP would be difficult to reconcile with objectives of nature preservation and restoration, as well as Earth system resilience.

The increase in M-COL resulting from the large-scale establishment of biomass plantations on former pastures can primarily be attributed to the higher amount of harvested NPP. At the same time, the prevented NPP through land use change decreases to some extent, as the higher productivity of the plantations compared to the pastures brings the global biosphere closer to its potential NPP. In line with that, the quantifications show a minor reduction in global M-COL under intensified management, as the NPP on plantations increases and only a fraction of it is harvested, allowing more energy to remain in the system (Figure 8). However, it needs to be evaluated to what degree the natural trophic system can utilize this energy and whether it can be considered a contribution to maintaining biosphere functioning or if it is instead preparing the soil for the next cultivation cycle and thereby contributing to the harvest.

In contrast to the findings for BECCS, the M-COL quantification indicates reforestation as an option to contribute to climate stabilization without further reducing the availability of photosynthetically derived energy for the biosphere. In the DC100 scenario, reforestation results in a negligible change of 0.13 Gt C yr^{-1} in M-COL compared to the land use reference and even -0.01 Gt C yr^{-1} for DC50 and -0.02 Gt C yr^{-1} for DC25. A marginal increase in M-COL can be explained by the representation of 30-year-old forests in LPJmL that show lower NPP than managed grasslands in some regions. While this may theoretically hold true for highly productive pastures, the dynamics need to be further evaluated for the affected regions. In the calculation of M-COL, this difference in NPP translates to an increase in prevented NPP, and thereby M-COL, despite minor reductions of harvested grass.
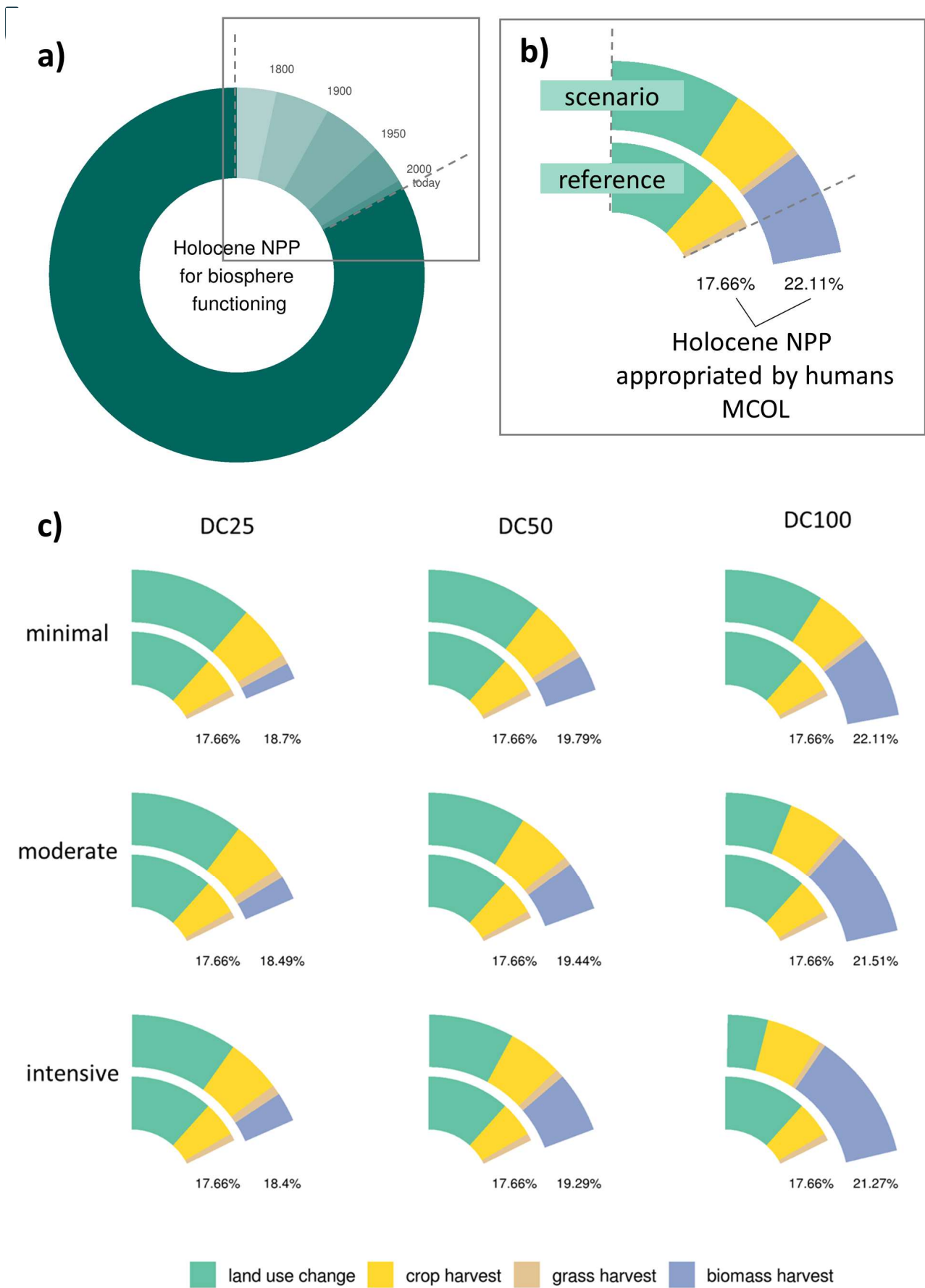
Figure 8. M-COL values as simulated by LPJmL for historic land use and different BECCS scenarios, showing a) the evolution of M-COL with resulting decreases in remaining Holocene-NPP for maintaining biosphere functions, b) only the NPP being appropriated by humans (M-COL) and its components for an exemplary scenario (DC100, minimal management) compared to the land use reference (land use of 2017 under future climate) c) the calculated M-COL values and components for the nine BECCS scenarios.

3.3 M-ECO evaluations of biosphere integrity

The quantification of M-ECO enabled the aggregation of key biospheric properties of the BECCS and reforestation scenarios in comparison to current land use. It is essential to consider the NETP-induced changes in M-ECO in light of the already significant biogeochemical, hydrological, and vegetation-structural modifications resulting from current land use. Human activities caused major ($0.3 < MECO > 0.6$) to severe (> 0.6) shifts in M-ECO on 3843 Mha of land, representing 26% of the global ice-free land surface (Figure 9).
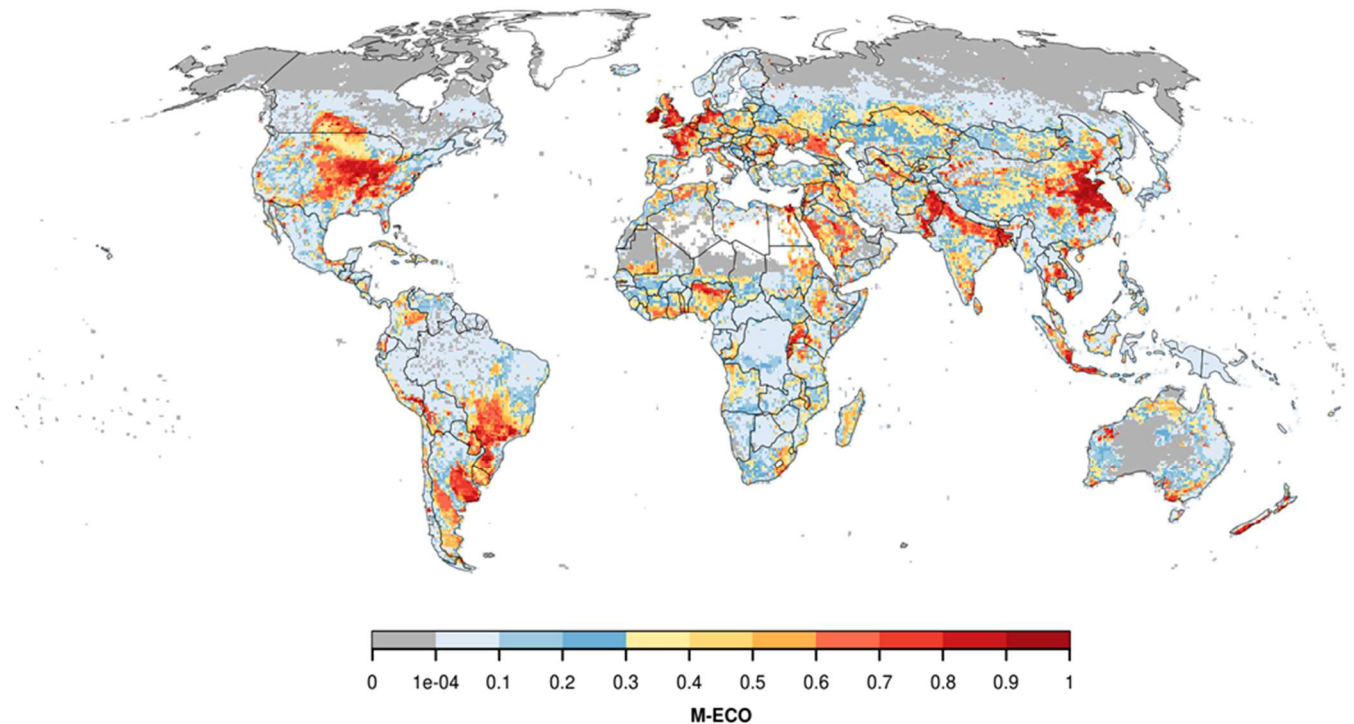

Figure 9. Global distribution of M-ECO (comprising structural and biogeochemical ecosystem changes) under current land use, showing major shifts compared to a scenario without human land use (>0.3) in yellow shades and severe shifts (>0.6) in red shades.

In the DC100 scenario, supplying BECCS feedstock under moderate management would risk to increase this highly impacted area by 9% or 338 Mha, covering in sum 29% (4181 Mha) of the global land surface. Notably, this includes a significant increase by 54% in the category of severe changes, translating to an additional 543 Mha globally (Figure 10 and Figure 11). In light of the already severe disruption of biosphere functionality caused by human activities today, careful consideration must be given to whether an expansion of such degree is justifiable.

By converting a smaller amount of pasture area to biomass plantations, the extent of additional major or severe shifts in M-ECO can be reduced. For instance, the implementation of DC25 would lead to a smaller expansion of 32 Mha and DC50 of 83 Mha of such shifts, assuming moderate management on plantations. Moreover, minimal management may lower the additional extent by 43% as compared to moderate management (+193Mha), whereas intensive management would increase the areas by almost 70% (+571 Mha) in the DC100 scenario. Nevertheless, it is important to note that regardless of the area of pasture rededication and management intensity, the BECCS scenarios entailed an expansion of highly disturbed systems in all cases.
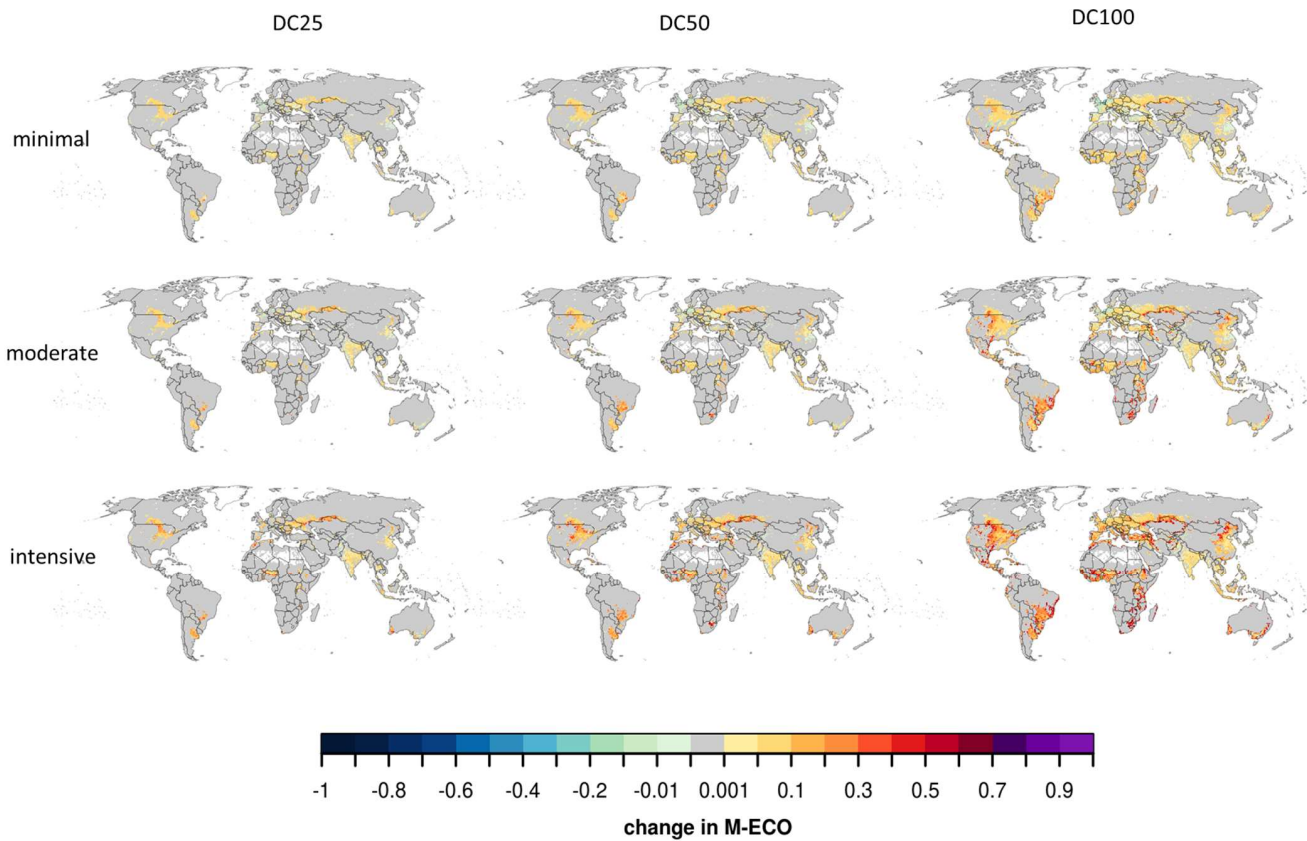
Figure 10. Shifts in M-ECO when transitioning from the land use reference to the different BECCS scenarios.

In contrast, reforestation contributes to climate stabilization, while significantly reducing M-ECO and thereby the pressure on biospheric functioning (Figure 12). The areas experiencing major shifts could be reduced by 346 Mha or 13% (DC100, 139 Mha for DC50, 39 Mha for DC25), reducing the global extent from 26% to 22% (Figure 11). Areas with severe shifts could be reduced by 121 Mha or 10% (DC100, 28 Mha for DC50, 6 Mha for DC25), resulting in a decline of the total extent from 8% to 6% of the global land surface, which compares to only half of the area affected severely in the BECCS scenario (Figure 11).

Biome-scale shifts in M-ECO

As indicated by significant reductions in M-ECO and most of its components aggregated to biome scale per continent in Figure 13, reforestation can contribute to restoring key properties of biomes. In general, the impact on M-ECO increases with higher grid cell fractions of land converted from managed grassland to forest (i.e. compare Figure 6 and Figure 12). When aggregated to biome level, the extent of the biome and the fraction of it being converted also play a role in the impact on M-ECO, i.e. the same reforested area having a greater impact on M-ECO for a biome of smaller extent. Therefore, the impact on the Asian coniferous forest (here referred to as plant composition of a boreal evergreen forest, but note the difference to the exclusion of the *climatic* boreal zone due to albedo effects) is relatively low, because only a small fraction of the overall extensive biome is converted. In contrast, the impact on the South American temperate forest is comparatively large, as a large share of a biome that is less dominant on the continent is reforested.
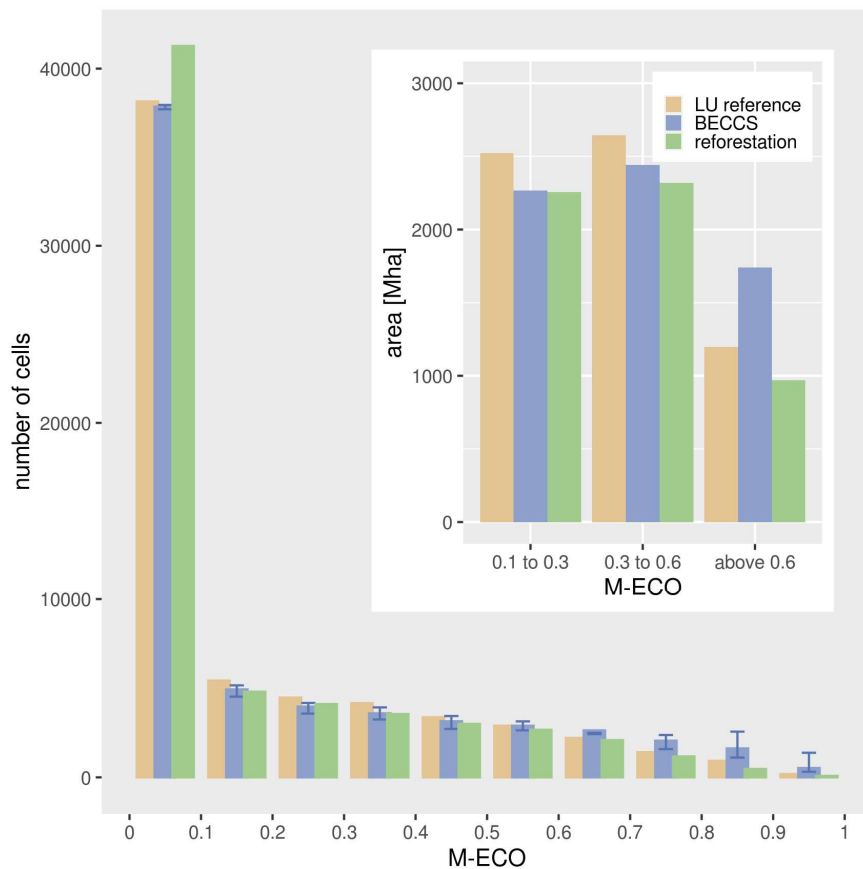
Figure 11. Distribution of M-ECO values a) among grid cells and b) aggregated to three bins (0.1–0.3 moderate shift, 0.3–0.6 major shift and >0.6 severe shift) and area covered by these M-ECO values. The error bars indicate the range between the minimal and intensive management scenarios for BECCS.

The majority of the biomes in Figure 13, which represent the two biomes per continent undergoing the largest conversion under the transition from the land use reference to the DC100 scenario, show substantial reductions in M-ECO. This implies that the majority of the biogeochemical, hydrological, and vegetation-structural properties assessed and aggregated in M-ECO would shift towards the Holocene state due to reforestation.

The decrease in M-ECO is mainly driven by changes in the vegetation structure, as the managed grassland shifts to a natural system (naturalness shifting from 0 to 1) of different plant functional types with structural attributes (i.e. evergreenness, needleleavedness, tropicalness, borealness) that are closer to the Holocene state. Furthermore, the carbon fluxes and stocks converge towards their natural state, as the distribution of carbon across the different pools as well as turnover rates begin to align with the dynamics of potential natural vegetation on the reforested areas. In addition, the cessation of grazing on these areas implies less carbon losses for the system. Due to these alterations in biomass accumulation as well as the absence of grazing animals consuming and releasing nitrogen in various forms, nitrogen flows and stocks are subject to some change, translating into minor to substantial shifts for different biomes. The water flows are only marginally affected, when aggregated to biome level. How these shifts in the key properties effect the local change component of M-ECO, varies between the biomes.

Regarding ecosystem balance, notable changes can be identified for temperate coniferous forests, which are also the most disturbed systems in the land use reference scenario, regarding this component. This implies that these

heavily impacted forest systems become more balanced in terms of relative magnitude among the property shifts (opposed to undermining the system's functionality by significant shifts in single flows/stocks) under reforestation. The impact of reforestation on the global importance component is however more pronounced in most cases. For the majority of the assessed biomes, the findings indicate a high global importance of the divergence from the Holocene state in the land use reference scenario. The BC100 reforestation scenario, however, results in a substantial reduction of this divergence, indicating that the contribution of reforestation to the restoration of the Holocene properties in forest ecosystems can potentially support global biosphere resilience. Assessing the overall impact of the aggregated M-ECO metric on the biome level, reveals that the temperate coniferous forest in Europe, North/Middle America and South America could even transition from a status of major to moderate shifts as compared to the stable Holocene state of the biome, if they were reforested according to the DC100 scenario.
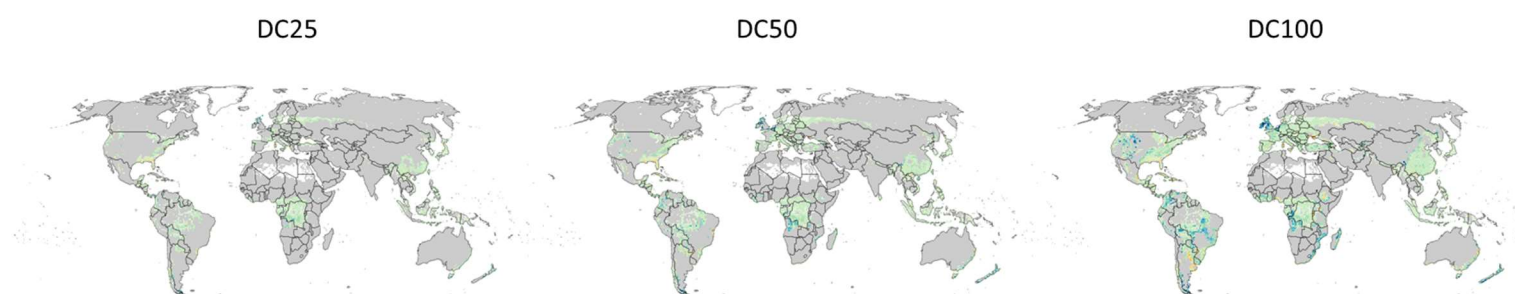
DC25	DC50	DC100

Figure 12. Shift in M-ECO when transitioning from the land use reference to the different reforestation scenarios.

In contrast to reforestation, BECCS leads to an increase in M-ECO for the most affected biomes (Figure 13). As the land allocation follows a different prioritization (i.e. favouring areas of high cropland share), the biomes with the largest area being rededicated are partly distinct to the biomes most affected by reforestation. As described above for reforestation, it holds true for BECCS: (i) the larger the area of conversion per cell, the larger the impact in the cell in general and (2) the larger the relative share of converted area within a biome, the larger the impact (i.e. compare Figure 6 and Figure 10). The greatest increase in M-ECO under the DC100 BECCS scenario with moderate management can be quantified for the South American temperate coniferous and tropical seasonal/deciduous forest, the North/Middle American temperate coniferous forest and the African warm woody savanna/woodland. While the amplifying effect of BECCS on M-ECO and its components is not as strong as the reduction through reforestation on the biome level, the quantification indicates an intensification of an already significant shift away from the Holocene state in the respective biomes.

The main drivers for the increase in M-ECO under the BECCS scenario are the more pronounced shifts away from the Holocene state for the carbon fluxes as well as nitrogen stocks and flows. Larger amounts of carbon are leaving the system through elevated harvests on biomass plantations compared to grazing systems, leading to a greater shift in carbon fluxes. The nitrogen components are mostly affected by the fertilization that is assumed for the plantation management of moderate intensity. Therefore, the impact on these three factors can be reduced by minimal management intensity, where no fertilizer is applied and the lower yields translate to less carbon losses for the system. Management intensification, in contrast, increases the shifts in carbon fluxes and nitrogen stocks and flows by higher yields and fertilizer rates. This increases M-ECO and results in significantly more severe M-ECO shifts than the moderate management (see upper end of the error bar in Figure 11).
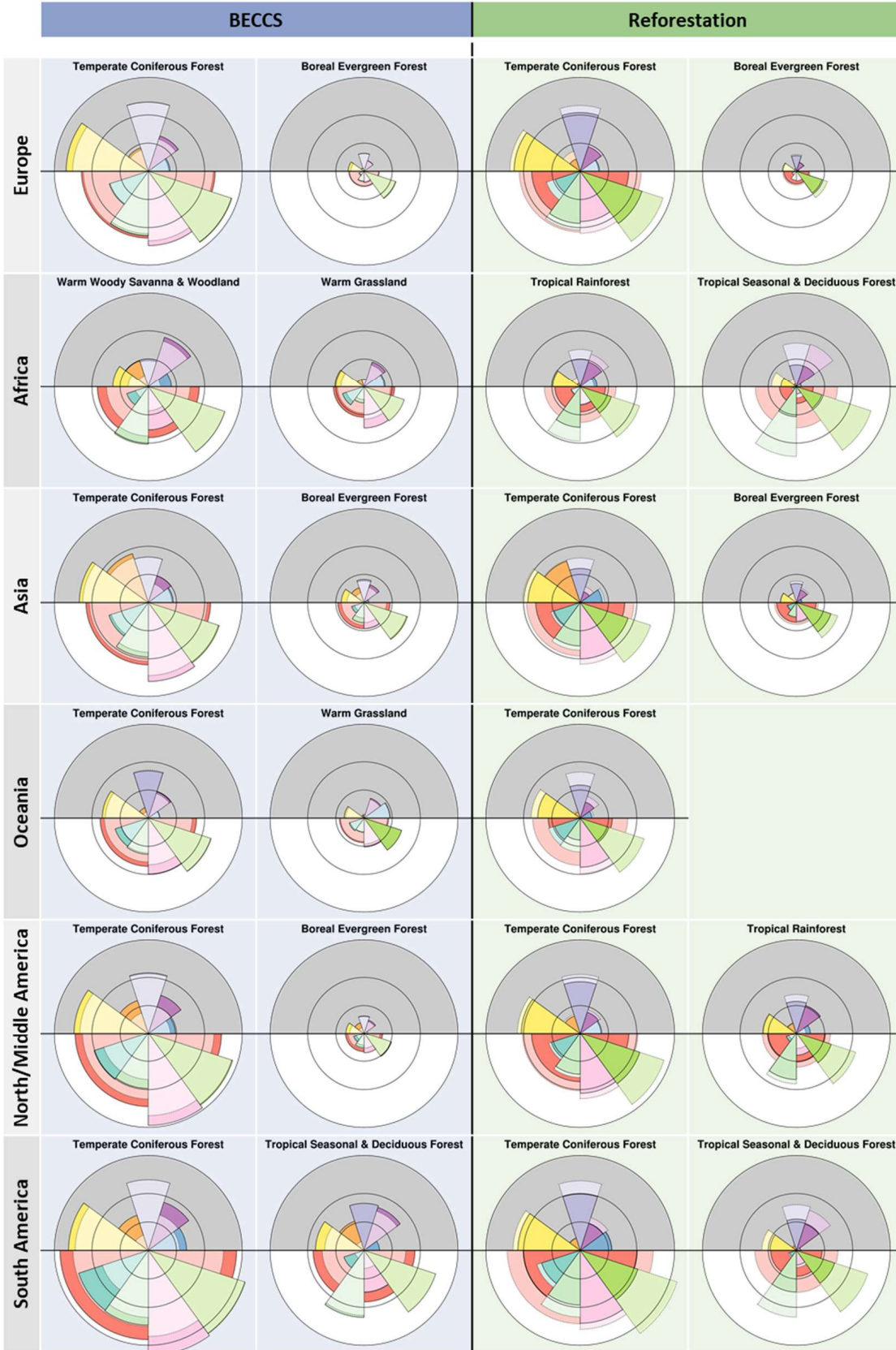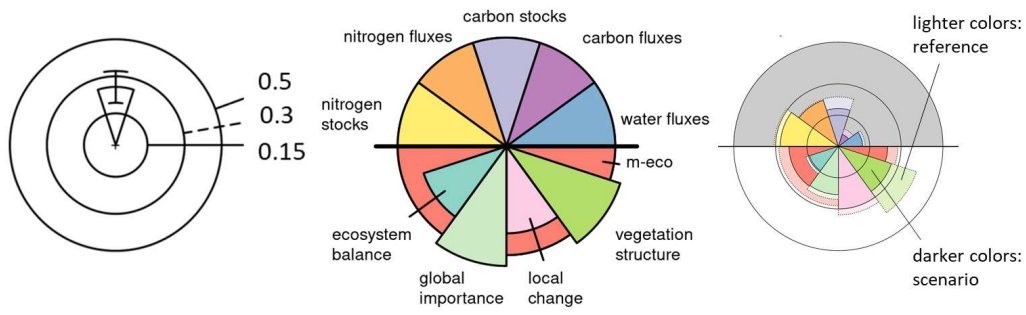
Figure 13.
Mean values for M-ECO and its components aggregated to biome level for the biomes with the largest area allocated for BECCS or reforestation per continent in the BC100 scenario.

29

NEGEM

4   *Discussion*

The findings of this deliverable emphasize the need for a comprehensive approach to climate and biosphere stewardship, as we show that the type and extent of NETP deployment have significant implications for biosphere integrity, with BECCS imposing greater pressure and reforestation alleviating it.

4.1   *CDR potentials for BECCS and reforestation*
[The contents of this section have been aligned with the corresponding section in the complementary Deliverable 3.7]

A shift towards a planetary health diet, as advocated by the EAT-Lancet commission, could potentially yield a reduction in grazing demand and consequently free up approximately 800 million hectares of pastureland. This area, equivalent to about 25% of the current global pasture areas, could then be utilized for BECCS feedstock production or reforestation. Utilizing these lands for biomass plantations to support BECCS could remove about 14.4 Gt CO_2eq yr-1 (9.7-18.5) through a biomass-to-electricity pathway, or approximately 8.9 Gt CO_2eq yr-1 (5.9-11.3) through biomass-to-liquid conversion, the latter being comparable to the median BECCS rates projected for 2100 in the economically optimized climate stabilization scenarios of the IPCC's AR6. These simulated sequestration rates correspond to approximately double the current global net carbon sink (1.9 GtC = 6.97 Gt CO_2) on the entire land surface for biomass-to-electricity, or slightly less than the global net carbon sink in oceans (2.9 GtC = 10.64 GtCO_2) for biomass-to-liquid (Friedlingstein et al., 2022), suggesting an anthropogenic sink that could be regarded as a form of bio-geoengineering of planetary scale (Heck et al., 2016).

Reforestation on pastures is found to yield a lower CDR per rededicated area when compared to BECCS, estimated at approximately 4.3 Gt CO_2eq yr-1 for a complete adoption of the planetary health diet. While the greater sequestration potential of BECCS might suggest the prioritization of BECCS over reforestation, the results of the impact assessment in Deliverable 3.7 and this report indicate that such a conclusion only holds from an isolated climate perspective. For further contextualization of CDR rates and interactions with the food system, see Deliverable 3.7. Complementary to this, the quantitative evaluation of functional biosphere integrity through process-based vegetation modelling is discussed in the following, providing additional information that is critical to consider when aiming for Earth system stability beyond climate stabilization.

4.2   *Implications of the findings from the biosphere integrity metrics*

BECCS
To assess the pressure on biosphere integrity through reducing photosynthetically derived energy availability for the biosphere, we computed M-COL under the different NETP scenarios. The use of land freed from pastures through a full transition to the planetary health diet for BECCS feedstock production was found to result in a significant increase in the appropriation of NPP by human activity, amounting to 21.27% of the Holocene NPP which is unavailable for the biosphere. This finding is alarming, as this measure alone could have the same impact as the total land use expansion and intensification observed over the past half-century. Such implications take on added significance when we consider the growing global demands for food and materials, in addition to BECCS.

Our findings further suggest that intensifying management practices may mitigate the impact on M-COL, as it leads to an increase in NPP, not all of which is harvested. However, it is important to note that this intensification causes substantial shifts among the components of the metric by increased harvesting and a higher proportion of managed NPP, which indicates significant transitions of the energy flows within the biosphere and thereby potentially disrupts essential processes (see 4.3).

Moreover, the BECCS scenarios demonstrate considerable alterations in essential biogeochemical, hydrological, and vegetation-structural characteristics of the biosphere, shown by the M-ECO assessment. These transitions would be imposed on a global landscape that has already significantly deviated from the stable Holocene state, which represents the full capacity to maintain Earth system resilience against abrupt and gradual abiotic changes. In this context, it needs to be carefully considered whether further pressures from BECCS are acceptable, given that many areas simulated to undergo the conversion from pasture to biomass plantation exhibit changes beyond the threshold of severe alteration (M-ECO > 0.6), which may lead to substantial disruption of fundamental processes. Additionally, the aggregation of these changes at the biome level highlights their significance, underscoring the large-scale impact of this transition beyond individual plantations. As the alterations of flows, stocks, and vegetation structure of all affected biomes is found to become more pronounced under BECCS deployment, it is emphasized that plantation-based NETPs are challenging to align with internationally agreed-upon targets for nature restoration, like Goal A of the Kunming-Montreal Global biodiversity framework calling for the "integrity, connectivity and resilience of all ecosystems ... [to be] maintained, enhanced, or restored" (CBD, 2022) by 2050.

While management intensification on plantations is found to increase the CDR potential, it also significantly increases the shifts away from the natural state, because the carbon and nitrogen fluxes are strongly altered. A reduction in agricultural inputs may on the other hand reduce the impacts to some degree, however also the sequestration potentials. Moreover, CDR magnitudes and impacts may be smaller for only partial transition to the planetary health diet. However, the impact assessments showed very clearly the direction of the effect on biosphere integrity being a reinforcement of already severe pressures.

Reforestation

In contrast to BECCS, reforestation provides a climate stabilization option without reducing the availability of photosynthetically derived energy for the biosphere required to maintain key functionalities, as demonstrated in the M-COL assessment. Complementary to that, the M-ECO evaluation indicates that reforestation can bring the ecosystem closer to the natural Holocene state in terms of fundamental properties of the vegetation structure and the carbon, nitrogen and water cycles. The global area experiencing major shifts in these attributes can be reduced from 18% to 16%, and the land experiencing severe shifts can be reduced from 8% to 6%, which is only half the area impacted that severely in the BECCS scenario. Furthermore, reforestation can contribute to restoring natural biogeochemical, hydrological and vegetation-structural properties of biomes to a substantial degree. In comparison, the approximation towards the Holocene state in the reforestation scenario was found to be considerably more prominent than the additional alleviation induced by the BECCS scenario. Therefore, the advantages of reforestation in terms of restoration are disproportionately higher than additional pressures by BECCS deployment, considering the environmental properties assessed in M-ECO.

These findings suggest that reforestation has the potential to make a significant contribution to the targets of the Kunming-Montreal Global Biodiversity Framework, specifically Target 2 to "[e]nsure that by 2030 at least 30 per cent of areas of degraded terrestrial, inland water, and coastal and marine ecosystems are under effective restoration ..." (CBD, 2022) and Target 3 to "[e]nsure and enable that by 2030 at least 30 per cent of terrestrial, inland water, and of coastal and marine areas, especially areas of particular importance for biodiversity and ecosystem functions and services, are effectively conserved ..." (CBD, 2022), especially when implemented as assisted regrowth opposed to forest plantations. Expanding protected areas by 736 Mha would raise the share of protected areas to approximately 22% of the Earth's land surface, from the current 16.6% (UNEP-WCMC et al., 2020). For a reference to EU policy, the results and reforestation strategies could further be linked to the EU's aim to plant three billion additional trees by 2030, which also addresses the interrelated challenges of climate change and biosphere degradation.

4.3 Suitability of the biosphere integrity metrics

This deliverable presents the first assessment of the effects of NETPs on functional biosphere integrity and demonstrates significant differences in the magnitude and direction of impacts between plantation-based BECCS and reforestation. By utilizing M-COL and M-ECO, we were able to quantitatively evaluate the implications of various future NETP deployment scenarios for functional biosphere integrity, surpassing qualitative appraisals. However, the analysis also exposed certain limitations to the application and interpretation of these metrics, which require transparent discussion.

M-COL

M-COL is designed to assess the functional biosphere integrity in terms of photosynthetically derived energy available for the biosphere to provide functional feedbacks in the Earth system. Given the focus on large-scale functionality, this metric is not intended to assess biodiversity or the disturbance of individual ecosystems.

Through the combination of prevented NPP through human activity and harvest into a single measure, M-COL tends to favor land sparing and intensification over land sharing and extensive management: if agricultural management is intensified on a specific area of land, the additional NPP can be harvested without any penalty for M-COL, assuming that the energy available for the biosphere remains constant. However, if residues (i.e. the NPP-fixed carbon remaining on the field after harvest) increase with elevated NPP and not all of the additional NPP is harvested, M-COL may even decrease, as found for the simulated biomass plantations in this analysis. However, it needs to be further assessed whether this energy is truly available to maintain key biosphere functions, or whether the residues rather prepare the soil for the subsequent cultivation cycle and ultimately support the next harvest.

If the carbon fixed by NPP that remains on the field after harvest was not considered available for maintaining biosphere functions, M-COL would not decrease with agricultural intensification, but stay constant. In this accounting, all additional NPP resulting from intensification would be considered as appropriated by humans, acknowledging that remaining residues do not contribute to functional integrity in the same way as NPP from non-managed systems. The reductions in M-COL that have been quantified for higher levels of management intensity in the BECCS scenarios of this analysis would not apply under such an adaption of the metric.

In addition to different approaches to account for energy flows within the metric, the interpretation of the results is critical for its applicability. Currently, we assess the share of Holocene NPP remaining available for providing key biosphere functions. However, it is unclear whether a critical threshold could be defined, i.e. what share of Holocene NPP can be appropriated by humans without risking disruption or degradation of biosphere functioning at a larger scale. Given that several indicators already show significant interference with the biosphere, it can be argued that such a threshold has already been transgressed. Therefore, the discussion on a limit to M-COL indicating an intact biosphere should focus on developing a restoration target. Discussing M-COL quantifications in relation to such a limit or restoration target would substantially increase the significance of the results. Furthermore, it would allow a quantitative assessment of the efforts to evolve towards biosphere stewardship involving nature restoration measures and responsible land management.

Currently, the utility of M-COL quantification lies in its ability to compare different scenarios and classify their interference strength in relation to historical trends. For BECCS in the pasture rededication scenario under the transition to the planetary health diet, we have thus calculated a vast increase in Holocene NPP appropriation comparable to the shift induced by the total land use over the last 50 years.

M-ECO

Complementary to the M-COL assessment, M-ECO addresses functional biosphere integrity by measuring changes in multiple biogeochemical stocks and fluxes, hydrological flows, and vegetation structure. With this range of evaluated properties, the metric is linked to more key processes than M-COL. Therefore, it is possible to identify the primary drivers of interference with the biosphere by examining the individual components of the metric. However, the complexity of aggregating the components, including their interrelationships (i.e., local change, ecosystem balance, global significance), presents a challenge for communicating the results.

As exemplified in this analysis, the results for M-ECO range from 0 to 1 and demand contextualization or categorization. In this study, the differentiation into moderate (>0.1 & < 0.3), major (>0.3 & <0.6) and severe (>0.6) alterations based on the biome shifts approach of Ostberg et al. (2013) was employed. Nevertheless, as argued for M-COL above, it would be valuable to introduce scientifically-based thresholds that signify distinct levels of risk for significant disruptions or degradation of functional biosphere integrity. This is particularly relevant as nitrogen dynamics have been integrated into the M-ECO metric by Stenzel et al. (2023) and yield a strong (potentially justified) response of the metric, which may necessitate a different approach for thresholds than the biome shift method used in this study and Ostberg et al. (2013).

Another crucial aspect in interpreting the M-ECO results is the appropriate level of spatial aggregation. The metric can in theory be used on the scale of single patches of land (e.g. a plantation) where it would indicate strong responses to most transitions. To evaluate the implications for biosphere integrity, the level of biomes is, however, more suitable (Steffen et al., 2015). A weak response of a biome if only a small fraction of it is (severely) changed, indicates that the biome is likely not compromised in its ability to sustain critical processes. This effect on the capacity to drive key ecological processes is essential when assessing functionality on a biosphere scale. Accordingly, alterations that result in substantial changes at the biome level represent a significant interference with the biosphere. In our analysis, we have identified such significant changes for multiple biomes in the NETP scenarios, indicating a more pronounced departure from the Holocene state for BECCS, and a partial restoration of it for reforestation. With this, our analysis has revealed contrasting effects of BECCS and reforestation, showing that the benefits of reforestation in terms of restoration are more pronounced than the negative impact of BECCS. While the lack of a scientifically-based threshold for contextualization of results of M-ECO remains a challenge, this quantitative comparison of scenarios has already expanded our analytical knowledge of NETP impacts on biosphere integrity.

4.4 Limitations of the analysis

The robustness of this quantitative assessment of NETP impacts on functional biosphere integrity may further be enhanced by an improved representation of reforestation in LPJmL. Our results suggest that the current approach of doubling the simulation period in order to reach the accumulation rates of aboveground biomass obtained from field measurements might still underestimate the recovery of soil carbon and vegetation carbon built-up on reforested areas. If the model would, however, indicate higher NPP in young forests, M-COL would be smaller in the reforestation scenarios, as the component of prevented NPP would decrease. Correspondingly, M-ECO would show lower levels of change than indicated by the current results, if the reforested areas were simulated to be closer to the maturity level of the natural state. Thus, the presented results for reforestation can be regarded as conservative estimates that are likely to show higher CDR potentials and stronger restoration effects for biosphere integrity with an improved representation of reforestation.

In addition, the model relies on input data from various sources (see Methods), with climate and land use inputs being the primary drivers for the M-COL and M-ECO outcomes. For this initial assessment, we have only examined model simulations based on data from one climate model of the CMIP6 ensemble providing climate data under RCP2.6 forcing. However, it is crucial to assess the uncertainty associated with the results when incorporating input from different climate models in future assessments. Furthermore, a larger number of distinct deployment pathways of the NETPs could be considered in subsequent evaluations. These could for example include other feedstocks for BECCS from agricultural and forestry residues or industrial and municipal point sources. Our assessment only considers dedicated biomass plantations that lead to relatively high impacts to highlight the significance of land use strategies involving BECCS. Additionally, in-depth assessments could explore the impact of timber harvest of different degrees on reforested areas, in contrast to the nature restoration approach of this study.

5   Key findings and policy relevant messages

[The contents of this section have been aligned with the corresponding section in the complementary Deliverable 3.7]

Transitioning to an EAT-Lancet planetary health diet could decrease the demand for grazing and release around 800 million hectares of pastureland that could be utilized for either reforestation or biomass plantations. If these areas were used for biomass plantations for BECCS, they could potentially remove approximately 14.4 $GtCO_2eq$ yr^{-1} if converted to electricity, or approximately 8.9 $GtCO_2eq$ yr^{-1} if converted to liquid, which is roughly equivalent to the median BECCS rates projected in 2100 in the economically optimized climate stabilization scenarios included in IPCC's AR6.

Such large-scale expansion of biomass plantations would however drastically interfere with the functional integrity of the biosphere, as this study demonstrates on a quantitative scale. Thus, establishing biomass plantations on pastures would reduce the energy available for the Earth system to maintain key biosphere functions by another 2.36 Gt C yr^{-1} on top of the already severe human appropriation of 11.26 Gt C yr^{-1}. This sums up to 21.27 % of the Holocene NPP being unavailable for the biosphere. Furthermore, it would increase the area that is subject to major or severe biogeochemical, hydrological and vegetation-structural shifts from 26% to 29% with the most affected biomes shifting even further away from the Holocene state than under current land use.

The levels of CDR and the environmental impacts are highly influenced by the management of biomass plantations. Increased irrigation and fertilization may lead to a higher CDR, but this can also amplify negative effects on crucial biosphere properties. Options to prevent these trade-offs would be precision farming, use of nitrification inhibitors, application of microbiome technology or breeding of species with enhanced tolerance towards water and nitrogen stress, which was beyond the scope of this assessment. The findings of our study highlight the risk of significant trade-off between CDR provision from dedicated biomass plantations for BECCS and other sustainability goals. To mitigate most of the side-effects, minimal management approaches such as rainfed and unfertilized plantations could be adopted, but this would require collective efforts for far-reaching political regulations in agricultural practices. Moreover, a partial shift to the EAT-Lancet planetary health diet may decrease the negative impacts as well as the CDR potential in magnitude, but the direction of the impacts would remain the same, thus adding pressure to an already distressed Earth system.

If the released pasture areas were reforested instead, less CO_2 would be removed per rededicated pasture area compared to BECCS, with a simulated CDR of ~4.3 $GtCO_2eq$ yr^{-1} for a full transition to the planetary health diet. This is higher than the median projected net removal on managed land for 2050 in 1.5°-2° compatible scenarios of IPCC's AR6, which mostly assume less stringent food system transformations, and similar to the median rates in 2100 (IPCC, 2022). In contrast to BECCS, however, reforestation provides an option to contribute to climate

stabilization without further reducing the availability of photosynthetically derived energy for the biosphere. In addition, the areas experiencing major shifts in key biospheric properties can be reduced from 18% to 16% and areas with severe shifts from 8% to 6%, which compares to half of the area affected severely in the BECCS scenario. By shifting elementary stocks, flows and structures back towards the natural state, reforestation can significantly contribute to restoring key properties at biome scale.

6   Conclusions and further steps

From a purely climate-focused perspective, dedicating pastures to biomass plantations for BECCS may be preferred over reforestation due to the higher levels of CDR and its permanence. However, this approach comes with significant trade-offs in terms of biosphere integrity, which is another crucial pillar of Earth system resilience. While reforestation entails some disadvantage over BECCS in regard of CDR, as it is a reversible option that saturates over time and is less efficient per area, it allows for the simultaneous support of achieving multiple sustainability targets by contributing to both climate stabilization and nature restoration. In terms of integrated climate stabilization and biosphere stewardship for the resilience of the entire Earth system, reforestation on pastures could thus be considered the preferable option, particularly for large-scale conversions and if extensive management on biomass plantations cannot be guaranteed globally.

This deliverable demonstrates that the metrics M-COL and M-ECO are suitable tools for comparing the impacts of two different land use intensive NETPs on biosphere integrity in a quantitative manner. The evaluation based on M-COL indicates that BECCS could decrease the availability of photosynthetically derived energy required for the biosphere to provide functional feedbacks in an already heavily stressed human-environment system, while the effects of reforestation are either insignificant or relieving the pressure. Complementing these findings, M-ECO involves a wider range of biogeochemical, hydrological and vegetation-structural properties that shift further away from the stable Holocene state under BECCS deployment, but can substantially be restored by large-scale reforestation. Overall, demonstrates on a quantitative scale that reforestation can add to climate stabilization while significantly contributing to the restoration of biosphere integrity, whereas BECCS may exacerbate the stress on biosphere integrity in an already severely strained system.

By enabling numerical assessments of biosphere integrity under different future scenarios, the metrics M-COL and M-ECO, therefore, qualify as tools to help identify and navigate development pathways that stabilize both the climate and biosphere as fundamental pillars of a functioning Earth system. Accordingly, they may contribute to coordinated efforts among science and policy that are required to develop strategies addressing the two intertwined crises of climate change and loss of biosphere integrity (Pörtner et al., 2023).

To support the success of this endeavour, this deliverable emphasizes the need for three actions:
(1) enhancing the NETP-specific process representation in vegetation modelling to extent the M-COL and M-ECO assessment to a wider range of NETPs beyond reforestation and plantation-based BECCS,
(2) scientific discussions on determining thresholds for interference with biosphere integrity, which indicate critical disruption of the Earth system's resilience, to be considered for restoration target setting and
(3) prioritizing policies that integrate climate stabilization and biosphere stewardship to account for their equally fundamental role for Earth system resilience.

The findings of this deliverable highlight the importance of multi-dimensional assessments for NETP deployment in the EU and beyond, considering all aspects of Earth system stability as well as socioeconomic effects. Coordinated efforts of science and policy are, thus, required to develop strategies that integrate urgently needed

(i) climate stabilization, (ii) nature restoration as well as (iii) food system transformations. To achieve this, the global perspective presented in this report needs to be complemented by analyses that focus on the specific conditions within EU countries, as envisioned in the objectives of the NEGEM project.

Incorporating the insights from this deliverable and its complementary counterpart (Deliverable 3.7), the synthesis report of WP3 (Deliverable 3.10) will integrate the impact assessments and evaluations of environmental constraints conducted within NEGEM. Furthermore, Deliverable 3.4 will assess the effects of climate extremes on NETP potentials, as the presented studies have thus far concentrated on low emission climate scenarios.

For preparing this report, the following deliverable/s have been taken into consideration:

D#	Deliverable title	Lead Beneficiary	Type	Dissemination level	Due date (in MM)
D3.1	Upgraded LPJmL5 version	PIK	R	PU	M12
D7.1	MONET-EU tool	ICL	R	PU	M12
D7.2	Extended MONET-EU	ICL	R	PU	M17
D3.2	Global NETP biogeochemical potential and impact analysis constrained by interacting planetary boundaries	PIK	R	PU	M24
D3.7	Global impacts on NETP potentials on food security and freshwater availability, scenario analysis of options and management choices	PIK	R	PU	M36

![NEGEM]

Appendix

S1. Revised parametrization of the herbaceous BFT

Within the NEGEM project, we have continuously worked on enhancing the representation of the above described carbon, nitrogen and water flows for the BFTs in LPJmL as a contribution to the core objective of NEGEM to assess realistic potentials of (biomass-based) NETPs. As part of these efforts, we have made some adaptations to the plant physiology and nitrogen distribution of the herbaceous BFT (see Table S 1). Specifically, we have adjusted the specific leaf area (i.e. the leaf extent per accumulated mass) to fit the reported value for Miscanthus in the TRY database, setting it to 39 mm^2 mg^{-1} dry matter (Kattge et al., 2020). In addition, we have modified the relation of leaf to root biomass from 0.75 to 2.50 to represent the high-growing Miscanthus, rather than regular C4 grass of significantly lower height. The adapted value falls within the narrow corridor of the complete coverage of different value ranges reported in the literature (Guo et al., 2016; Rakić et al., 2021; Trybula et al., 2015) (Table S 1).

In terms of biomass decay, we have further suppressed the natural turnover of leaf biomass to the litter pool in the model, as this biomass is typically harvested in managed systems. Opposed to the former harvest routine depending on carbon accumulation, the harvest has been set to a single event per year (Table S 1)Table S 1 to better represent the common practice (Li et al., 2018). Moreover, we have adapted the C/N ratio of the aboveground biomass to match the measurements by Heaton et al. (2009), using the interannual variance to determine minimum, median, and maximum ratios in the model (Table S 1). Finally, we have also adjusted the nitrogen recovery rate based on measurements of the nitrogen content in standing biomass from the same publication, setting it to 32% for green harvest and 70% for brown harvest (Heaton et al., 2009). However, this assessment exclusively assumes green harvest as it is reported a common practice (Li et al., 2018) and allows for processing to biofuels (Winkler et al., 2020).

Table S 1. Adjustments of parameters of the herbaceous bioenergy functional type.

Parameter	Default value	Adjusted value	Literature
Specific leaf area	23 mm^2 mg^{-1} dry matter	39 mm^2 mg^{-1} dry matter	10–70 mm^2 mg^{-1} dry matter (Cheng et al., 2020) 11–99 mm^2 mg^{-1} dry matter (Kattge et al., 2020)
Ratio of leaf biomass to root biomass	0.75	2.50	1.04–1.31 at emergence (Trybula et al., 2015) 4.55-8.33 at maturity (Trybula et al., 2015) 2.31–4.54 (Guo et al., 2016) 1.43–2.50 (Rakić et al., 2021)
turnover	$\frac{1}{365}$ leaf mass per day	none	
Harvest date	Determined by carbon accumulation	*Northern hemisphere:* 1. Oct. for green harvest 1. Feb. for brown harvest *Southern hemisphere:* 1. Apr. for green harvest 1. Aug. for brown harvest	*Northern hemisphere:* All months covered without distinction for green and brown harvest in Li et al. (2018) October for green harvest (Winkler et al., 2020) March for brown harvest (Winkler et al., 2020)
C/N ratio in leaves	Median: 34.0 minimum: 17.4 Maximum: 66.9	Median: 90 minimum: 34 maximum: 132	34–132 (Heaton et al., 2009)
N recovery	70%	Green harvest: 31.80% brown harvest: 70.12%	31.80–70.12% (Heaton et al., 2009)

Table S 2. PFT-specific attributes for vegetation structure from Stenzel et al. (2023).

	trees				
name	evergreen-ness	needleleaved-ness	tropical-ness	boreal-ness	natural-ness
Tropical broadleaved evergreen	1	0	1	0	1
Tropical broadleaved raingreen	0	0	1	0	1
Temperate needleleaved evergreen	1	1	0	0	1
Temperate broadleaved evergreen	1	0	0	0	1
Temperate broadleaved summergreen	0	0	0	0	1
Boreal needleleaved evergreen	1	1	0	1	1
Boreal broadleaved summergreen	0	0	0	1	1
Boreal needleleaved summergreen	0	1	0	1	1
Tropical bioenergy rainfed	1	0	1	0	0
Temperate bioenergy rainfed	0	0	0	0	0
Tropical bioenergy irrigated	1	0	1	0	0
Temperate bioenergy irrigated	0	0	0	0	0

	grasses/crops		
	tropicalness	borealness	naturalness
C4 grass tropic	1	0	1
C3 grass temperate	0	0	1
C3 grass polar	0	1	1
Temperate cereals	0	0	0
Rice	1	0	0
Maize	1	0	0
Tropical cereals	1	0	0
Pulses	0.5	0	0
Temperate roots	0	0	0
Tropical roots	1	0	0
Sunflower	0.5	0	0
Soybean	1	0	0
Groundnut	1	0	0
Rapeseed	0.5	0	0
Sugarcane	1	0	0
Others	0.5	0	0
Managed grass	dyn*	dyn*	0
Bioenergy grass	1	0	0
Grass under bioenergy trees	dyn*	dyn*	0

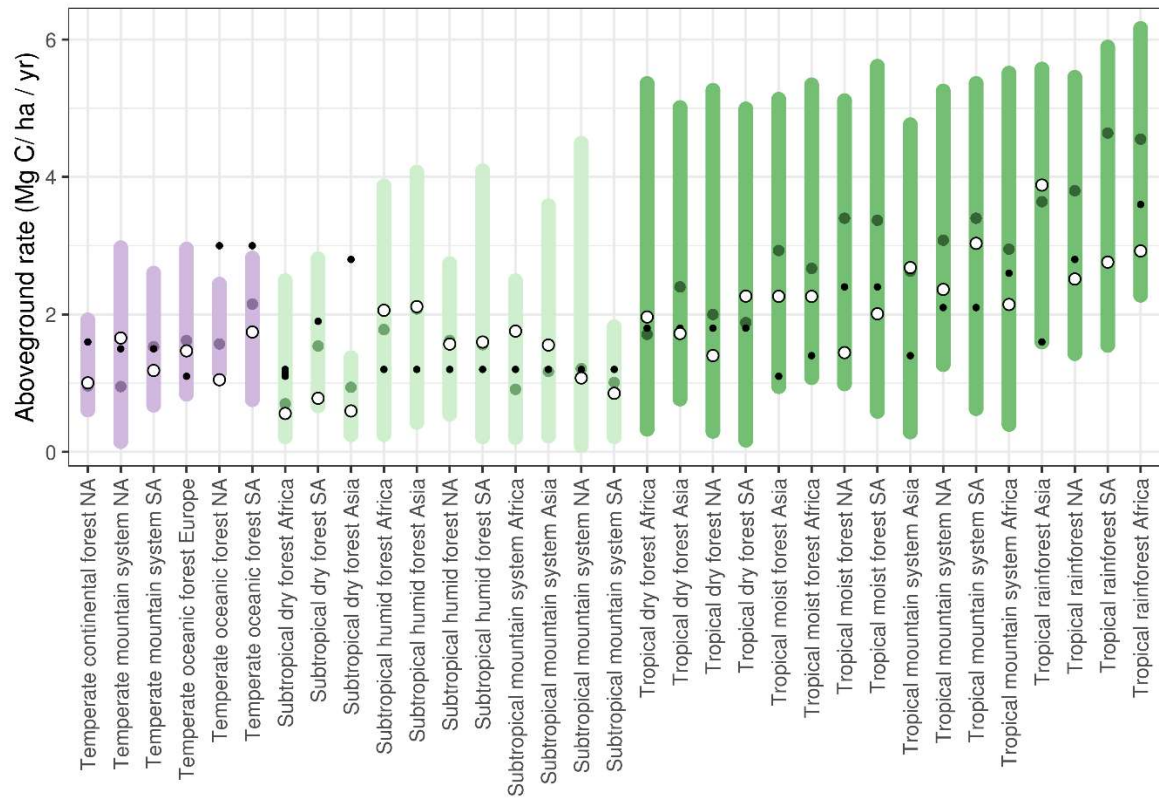* dynamic share due to climate specific grass mix

Figure S 1: Comparison of simulated median aboveground carbon accumulation rates (open circles) per ecozone to (i) IPCC (2019) defaults (filled black circles) and (ii) predicted rates from Cook-Patton et al. (2020) (coloured circles for the average and coloured bars for the range between minimum and maximum simulated rate). Simulated rates refer to the assumption that carbon pools after 60 years of simulation with LPJmL are reached within 30 years to compensate for too slow establishment rates. NA = North America; SA = South America.
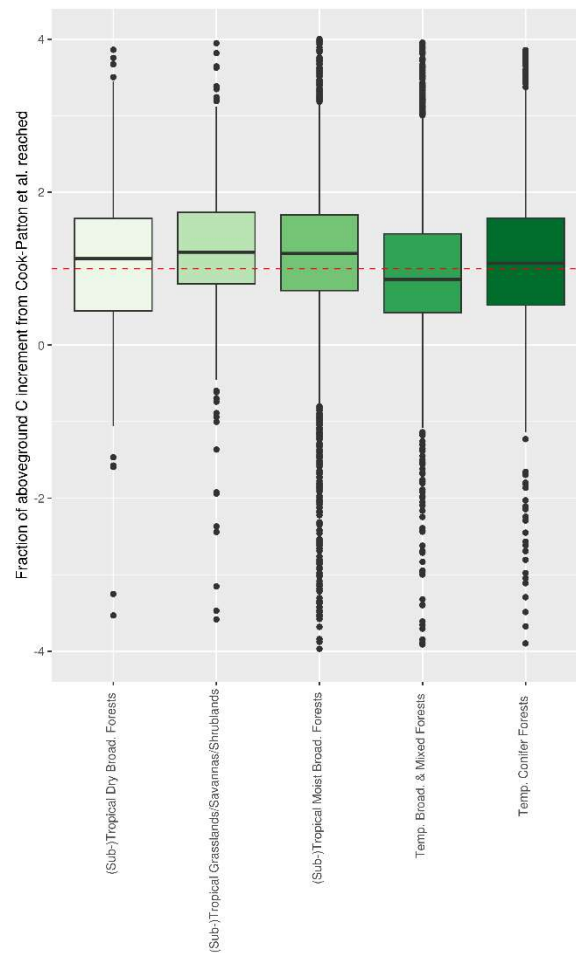
Figure S 2 The fraction of aboveground carbon increment given for reforestation on pastures for five biomes in Cook-Patton et al. (2020) reached by LPJmL simulations over 60 years. The dotted red line highlights the value of 1 which represents a complete resemblance of the observed data.
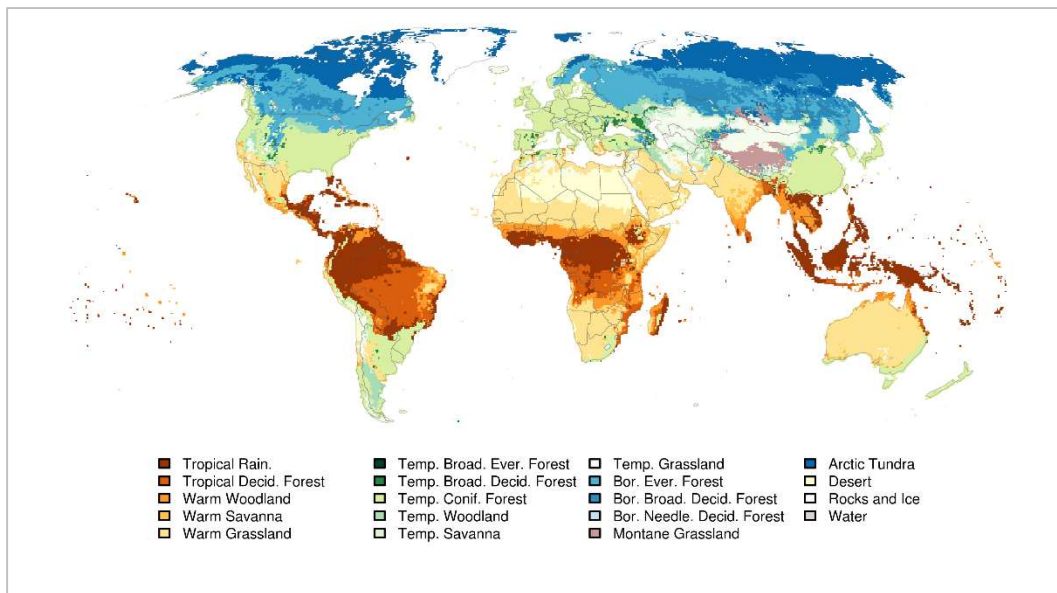
Figure S 3: Biomes based on simulated distribution of plant functional types in LPJmL (for potential natural vegetation under 2036-2065 climate for RCP2.6-SSP1).
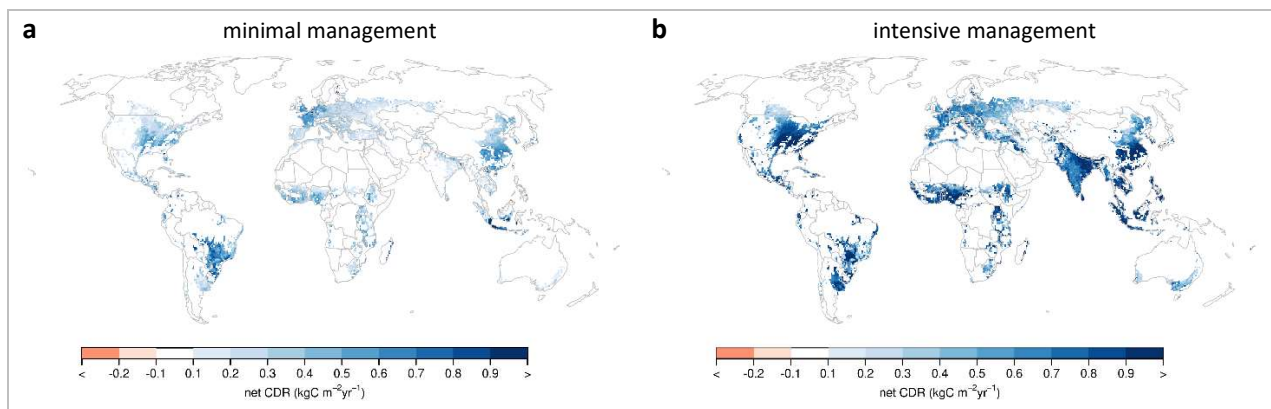

Figure S 4: Simulated net CDR from biomass plantations for BECCS assuming (a) minimal management and (b) intensive management, as well as a B2E pathway.
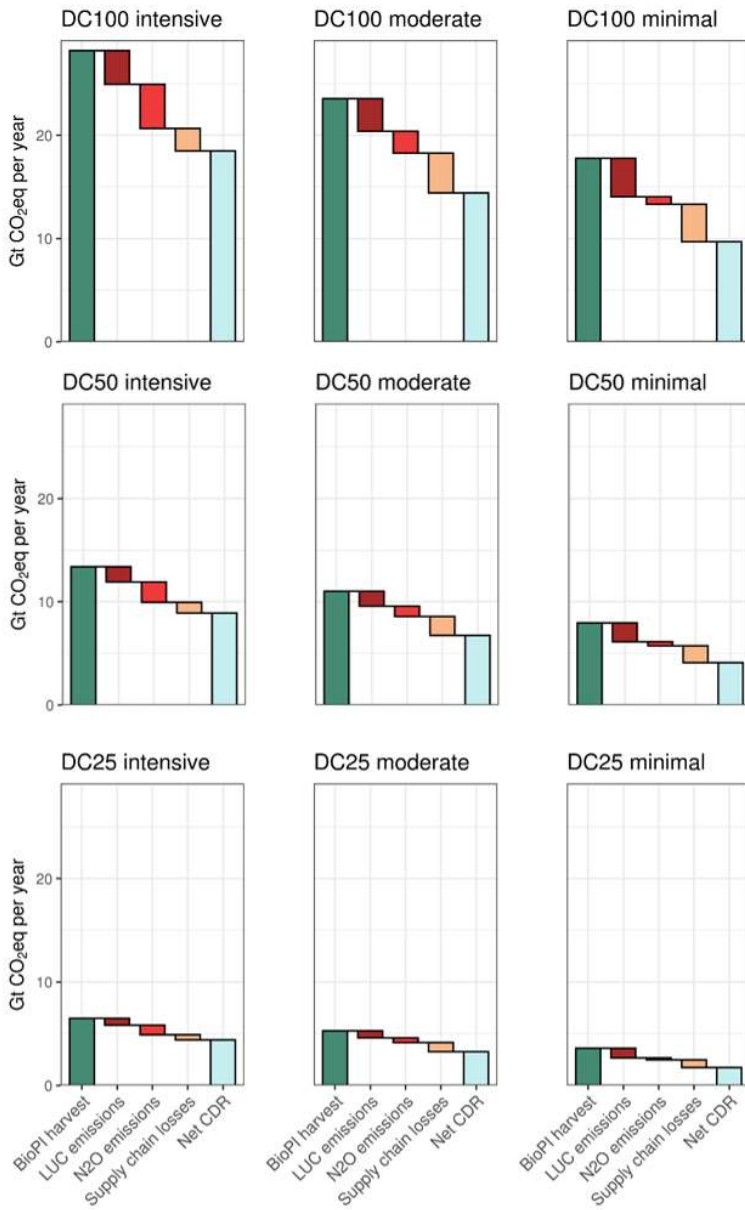
Figure S 5: Calculation of global net CDR from rededicated pastures to biomass plantations for BECCS, for partial or full transition to EAT-Lancet diet (DC25, DC50, DC100) and three management scenarios (intensive, moderate and minimal). Harvested CO_2eq are reduced by land use change emissions through reduced carbon pools on plantations (dark red), additional N_2O emissions through fertilization on plantations (in CO_2eq; red), and CO_2 losses along the BECCS supply chain through fossil fuel use and in the carbon capture and storage process (orange, here for a B2E pathway; see methods).

References

Aragão, L. E. O. C. (2012). The rainforest's water pump. *Nature*, *489*(7415), 217-218. https://doi.org/10.1038/nature11485

Bai, Y., & Cotrufo, M. F. (2022). Grassland soil carbon sequestration: Current understanding, challenges, and solutions. *Science*, *377*(6606), 603-608. https://doi.org/doi:10.1126/science.abo2380

Benton, T. G., Bieg, C., Harwatt, H., Pudasaini, R., & Wellesley, L. (2021). *Food system impacts on biodiversity loss. Three levers for food system transformation in support of nature.*

Betts, M. G., Wolf, C., Ripple, W. J., Phalan, B., Millers, K. A., Duarte, A., Butchart, S. H. M., & Levi, T. (2017). Global forest loss disproportionately erodes biodiversity in intact landscapes. *Nature*, *547*(7664), 441-444. https://doi.org/10.1038/nature23285

Bonan, G. B. (2008). Forests and Climate Change: Forcings, Feedbacks, and the Climate Benefits of Forests. *Science*, *320*(5882), 1444-1449. https://doi.org/doi:10.1126/science.1155121

Boysen, L. R., Lucht, W., & Gerten, D. (2017). Trade-offs for food production, nature conservation and climate limit the terrestrial carbon dioxide removal potential. *Global Change Biology*, *23*(10), 4303-4317. https://doi.org/10.1111/gcb.13745

Braun, J., Werner, C., Lucht, W., & Gerten, D. (2022). *Global NETP biogeochemical potential and impact analysis constrained by interacting planetary boundaries (D3.2).*

Campbell, B. M., Beare, D. J., Bennett, E. M., Hall-Spencer, J. M., Ingram, J. S. I., Jaramillo, F., Ortiz, R., Ramankutty, N., Sayer, J. A., & Shindell, D. (2017). Agriculture production as a major driver of the Earth system exceeding planetary boundaries. *Ecology and Society*, *22*(4), Article 8. https://doi.org/10.5751/ES-09595-220408

CBD. (2022). Kunming-Montreal Global Biodiversity Framework. Montreal.

Chen, C., Chaudhary, A., & Mathys, A. (2022). Dietary Change and Global Sustainable Development Goals [Review]. *Frontiers in Sustainable Food Systems*, *6*. https://doi.org/10.3389/fsufs.2022.771041

Cheng, Y., Huang, M., Chen, M., Guan, K., Bernacchi, C., Peng, B., & Tan, Z. (2020). Parameterizing Perennial Bioenergy Crops in Version 5 of the Community Land Model Based on Site-Level Observations in the Central Midwestern United States. *Journal of Advances in Modeling Earth Systems*, *12*(1), e2019MS001719. https://doi.org/https://doi.org/10.1029/2019MS001719

Chiquier, S., Patrizio, P., Bui, M., Sunny, N., & Mac Dowell, N. (2022). A comparative analysis of the efficiency, timing, and permanence of CO2 removal pathways [10.1039/D2EE01021F]. *Energy & Environmental Science*, *15*(10), 4389-4403. https://doi.org/10.1039/D2EE01021F

Chiquier, S., Patrizio, P., Sunny, N., & Mac Dowell, N. (2022). *Link MONET-EU and JEDI (D7.3).*

Conant, R. T., Paustian, K., & Elliott, E. T. (2001). GRASSLAND MANAGEMENT AND CONVERSION INTO GRASSLAND: EFFECTS ON SOIL CARBON. *Ecological Applications*, *11*(2), 343-355. https://doi.org/https://doi.org/10.1890/1051-0761(2001)011[0343:GMACIG]2.0.CO;2

Cook-Patton, S. C., Leavitt, S. M., Gibbs, D., Harris, N. L., Lister, K., Anderson-Teixeira, K. J., Briggs, R. D., Chazdon, R. L., Crowther, T. W., Ellis, P. W., Griscom, H. P., Herrmann, V., Holl, K. D., Houghton, R. A., Larrosa, C., Lomax, G., Lucas, R., Madsen, P., Malhi, Y., . . . Griscom, B. W. (2020). Mapping carbon accumulation potential from global natural forest regrowth. *Nature*, *585*(7826), 545-550. https://doi.org/10.1038/s41586-020-2686-x

Cook, R. L., Stape, J. L., & Binkley, D. (2014). Soil Carbon Dynamics Following Reforestation of Tropical Pastures. *Soil Science Society of America Journal*, *78*(1), 290-296. https://doi.org/https://doi.org/10.2136/sssaj2012.0439

de Koning, G. H. J., Veldkamp, E., & López-Ulloa, M. (2003). Quantification of carbon sequestration in soils following pasture to forest conversion in northwestern Ecuador. *Global Biogeochemical Cycles*, *17*(4). https://doi.org/https://doi.org/10.1029/2003GB002099

Exposito-Alonso, M., Booker, T. R., Czech, L., Gillespie, L., Hateley, S., Kyriazis, C. C., Lang, P. L. M., Leventhal, L., Nogues-Bravo, D., Pagowski, V., Ruffley, M., Spence, J. P., Toro Arana, S. E., Weiß, C. L., & Zess, E. (2022). Genetic diversity loss in the Anthropocene. *Science*, *377*(6613), 1431-1435. https://doi.org/doi:10.1126/science.abn5642

FAO. (2023). *Food Balance Sheets*. https://www.fao.org/faostat/en/#data/FBS

Fearnside, P. M., & Imbrozio Barbosa, R. (1998). Soil carbon changes from conversion of forest to pasture in Brazilian Amazonia. *Forest Ecology and Management*, *108*(1), 147-166. https://doi.org/https://doi.org/10.1016/S0378-1127(98)00222-9

Folke, C., Jansson, Å., Rockström, J., Olsson, P., Carpenter, S. R., Chapin, F. S., Crépin, A.-S., Daily, G., Danell, K., Ebbesson, J., Elmqvist, T., Galaz, V., Moberg, F., Nilsson, M., Österblom, H., Ostrom, E., Persson, Å., Peterson, G., Polasky, S., . . . Westley, F. (2011). Reconnecting to the Biosphere. *Ambio*, *40*(7), 719-738. https://doi.org/10.1007/s13280-011-0184-y

Friedlingstein, P., O'Sullivan, M., Jones, M. W., Andrew, R. M., Gregor, L., Hauck, J., Le Quéré, C., Luijkx, I. T., Olsen, A., Peters, G. P., Peters, W., Pongratz, J., Schwingshackl, C., Sitch, S., Canadell, J. G., Ciais, P., Jackson, R. B., Alin, S. R., Alkama, R., . . . Zheng, B. (2022). Global Carbon Budget 2022. *Earth Syst. Sci. Data*, *14*(11), 4811-4900. https://doi.org/10.5194/essd-14-4811-2022

Friggens, N. L., Hester, A. J., Mitchell, R. J., Parker, T. C., Subke, J.-A., & Wookey, P. A. (2020). Tree planting in organic soils does not result in net carbon sequestration on decadal timescales. *Global Change Biology*, *26*(9), 5178-5188. https://doi.org/https://doi.org/10.1111/gcb.15229

Guo, H., Hong, C., Chen, X., Xu, Y., Liu, Y., Jiang, D., & Zheng, B. (2016). Different Growth and Physiological Responses to Cadmium of the Three Miscanthus Species. *Plos One*, *11*(4), e0153475. https://doi.org/10.1371/journal.pone.0153475

Haberl, H., Erb, K. H., Krausmann, F., Gaube, V., Bondeau, A., Plutzar, C., Gingrich, S., Lucht, W., & Fischer-Kowalski, M. (2007). Quantifying and mapping the human appropriation of net primary production in earth's terrestrial ecosystems. *Proceedings of the National Academy of Sciences*, *104*(31), 12942-12947. https://doi.org/10.1073/pnas.0704243104

Hanssen, S. V., Daioglou, V., Steinmann, Z. J. N., Frank, S., Popp, A., Brunelle, T., Lauri, P., Hasegawa, T., Huijbregts, M. A. J., & Van Vuuren, D. P. (2020). Biomass residues as twenty-first century bioenergy feedstock—a comparison of eight integrated assessment models. *Climatic Change*, *163*(3), 1569-1586. https://doi.org/10.1007/s10584-019-02539-x

Heaton, E. A., Dohleman, F. G., & Long, S. P. (2009). Seasonal nitrogen dynamics of Miscanthus×giganteus and Panicum virgatum [https://doi.org/10.1111/j.1757-1707.2009.01022.x]. *GCB Bioenergy*, *1*(4), 297-307. https://doi.org/https://doi.org/10.1111/j.1757-1707.2009.01022.x

Heck, V., Gerten, D., Lucht, W., & Boysen, L. R. (2016). Is extensive terrestrial carbon dioxide removal a 'green' form of geoengineering? A global modelling study. *Global and Planetary Change*, *137*, 123-130. https://doi.org/10.1016/j.gloplacha.2015.12.008

Heck, V., Gerten, D., Lucht, W., & Popp, A. (2018). Biomass-based negative emissions difficult to reconcile with planetary boundaries. *Nature Climate Change*, *8*(2), 151-155. https://doi.org/10.1038/s41558-017-0064-y

Heinke, J., Rolinski, S., & Müller, C. (2022). Modeling the role of livestock grazing in C and N cycling in grasslands with LPJmL5.0-grazing. *Geosci. Model Dev. Discuss.*, *2022*, 1-31. https://doi.org/10.5194/gmd-2022-176

Herrero, M., Havlík, P., Valin, H., Notenbaert, A., Rufino, M. C., & Thornton, P. K. (2013). Biomass use, production, feed efficiencies, and greenhouse gas emissions from global livestock systems. *Proc Natl Acad Sci USA*, *110*. https://doi.org/10.1073/pnas.1308149110

Heyder, U., Schaphoff, S., Gerten, D., & Lucht, W. (2011). Risk of severe climate change impact on the terrestrial biosphere. *Environmental Research Letters*, *6*(3). https://doi.org/Artn03403610.1088/1748-9326/6/3/034036

Humpenöder, F., Popp, A., Bodirsky, B. L., Weindl, I., Biewald, A., Lotze-Campen, H., Dietrich, J. P., Klein, D., Kreidenweis, U., Müller, C., Rolinski, S., & Stevanovic, M. (2018). Large-scale bioenergy production: how to resolve sustainability trade-offs? *Environmental Research Letters*, *13*(2), 024011. https://doi.org/10.1088/1748-9326/aa9e3b

IPBES. (2019). *Global assessment report on biodiversity and ecosystem services of the Intergovernmental Science-Policy Platform on Biodiversity and Ecosystem Service*. Intergovernmental Science-Policy Platform on Biodiversity and Ecosystem Service. https://doi.org/10.5281/zenodo.3831673

IPCC. (2019). *Refinement to the 2006 IPCC Guidelines for National Greenhouse Gas Inventories. Volume 4: Agriculture, Forestry and Other Land Use*.

IPCC. (2022). *Climate Change 2022. Mitigation of Climate Change. Working Group III contribution to the Sixth Assessment Report of the Intergovernmental Panel on Climate Change*. Cambridge University Press. https://doi.org/10.1017/9781009157926

Jägermeyr, J., Gerten, D., Heinke, J., Schaphoff, S., Kummu, M., & Lucht, W. (2015). Water savings potentials of irrigation systems: global simulation of processes and linkages. *Hydrology Earth System Sciences*, *19*(7), 3073-3091. https://doi.org/10.5194/hess-19-3073-2015

Kattge, J., Bönisch, G., Díaz, S., Lavorel, S., Prentice, I. C., Leadley, P., Tautenhahn, S., Werner, G. D. A., Aakala, T., Abedi, M., Acosta, A. T. R., Adamidis, G. C., Adamson, K., Aiba, M., Albert, C. H., Alcántara, J. M., Alcázar C, C., Aleixo, I., Ali, H., . . . Wirth, C. (2020). TRY plant trait database – enhanced coverage and open access. *Global Change Biology*, *26*(1), 119-188. https://doi.org/https://doi.org/10.1111/gcb.14904

Kirschbaum, M. U. F., Guo, L. B., & Gifford, R. M. (2008). Why does rainfall affect the trend in soil carbon after converting pastures to forests?: A possible explanation based on nitrogen dynamics. *Forest Ecology and Management*, *255*(7), 2990-3000. https://doi.org/https://doi.org/10.1016/j.foreco.2008.02.005

Lange, S. (2019). *WFDE5 over land merged with ERA5 over the ocean (W5E5). V. 1.0.* https://doi.org/10.5880/pik.2019.023

Lange, S., & Büchner, M. (2021). *ISIMIP3b bias-adjusted atmospheric climate input data (v1.1). ISIMIP Repository* Version 1.1). https://doi.org/10.48364/ISIMIP.842396.1

Leblanc, F., Bibas, R., Mima, S., Muratori, M., Sakamoto, S., Sano, F., Bauer, N., Daioglou, V., Fujimori, S., Gidden, M. J., Kato, E., Rose, S. K., Tsutsui, J., van Vuuren, D. P., Weyant, J., & Wise, M. (2022). The contribution of bioenergy to the decarbonization of transport: a multi-model assessment. *Climatic Change*, *170*(3), 21. https://doi.org/10.1007/s10584-021-03245-3

Li, W., Ciais, P., Makowski, D., & Peng, S. (2018). A global yield dataset for major lignocellulosic bioenergy crops based on field measurements. *Scientific Data*, *5*(1), 180169. https://doi.org/10.1038/sdata.2018.169

Newbold, T. (2018). Future effects of climate and land-use change on terrestrial vertebrate community diversity under different scenarios. *Proceedings of the Royal Society B: Biological Sciences*, *285*(1881), 20180792. https://doi.org/doi:10.1098/rspb.2018.0792

Ostberg, S., Boysen, L. R., Schaphoff, S., Lucht, W., & Gerten, D. (2018). The Biosphere Under Potential Paris Outcomes. *Earth's Future*, *6*(1), 23-39. https://doi.org/https://doi.org/10.1002/2017EF000628

Ostberg, S., Lucht, W., Schaphoff, S., & Gerten, D. (2013). Critical impacts of global warming on land ecosystems. *Earth System Dynamics*, *4*(2), 347-357. https://doi.org/10.5194/esd-4-347-2013

Ostberg, S., Müller, C., Heinke, J., & Schaphoff, S. (2023). LandInG 1.0: A toolbox to derive input datasets for terrestrial ecosystem modelling at variable resolutions from heterogeneous sources. *Geosci. Model Dev. Discuss.*, *2023*, 1-46. https://doi.org/10.5194/gmd-2022-291

Pongratz, J., Reick, C. H., Raddatz, T., Caldeira, K., & Claussen, M. (2011). Past land use decisions have increased mitigation potential of reforestation. *Geophysical Research Letters*, *38*, n/a-n/a. https://doi.org/10.1029/2011GL047848

Pörtner, H.-O., Scholes, R. J., Arneth, A., Barnes, D. K. A., Burrows, M. T., Diamond, S. E., Duarte, C. M., Kiessling, W., Leadley, P., Managi, S., McElwee, P., Midgley, G., Ngo, H. T., Obura, D., Pascual, U., Sankaran, M., Shin, Y. J., & Val, A. L. (2023). Overcoming the coupled climate and biodiversity crises and their societal impacts. *Science*, *380*(6642), eabl4881. https://doi.org/doi:10.1126/science.abl4881

Rakić, T., Pešić, M., Kostić, N., Andrejić, G., Fira, D., Dželetović, Ž., Stanković, S., & Lozo, J. (2021). Rhizobacteria associated with Miscanthus x giganteus improve metal accumulation and plant growth in the flotation tailings. *Plant and Soil*, *462*(1), 349-363. https://doi.org/10.1007/s11104-021-04865-5

Riggio, J., Baillie, J. E. M., Brumby, S., Ellis, E., Kennedy, C. M., Oakleaf, J. R., Tait, A., Tepe, T., Theobald, D. M., Venter, O., Watson, J. E. M., & Jacobson, A. P. (2020). Global human influence maps reveal clear

opportunities in conserving Earth's remaining intact terrestrial ecosystems. *Global Change Biology*, *26*(8), 4344-4356. https://doi.org/https://doi.org/10.1111/gcb.15109

Rockström, J., Beringer, T., Hole, D., Griscom, B., Mascia, M. B., Folke, C., & Creutzig, F. (2021). We need biosphere stewardship that protects carbon sinks and builds resilience. *Proceedings of the National Academy of Sciences*, *118*(38), e2115218118. https://doi.org/doi:10.1073/pnas.2115218118

Rose, S. K., Popp, A., Fujimori, S., Havlik, P., Weyant, J., Wise, M., van Vuuren, D., Brunelle, T., Cui, R. Y., Daioglou, V., Frank, S., Hasegawa, T., Humpenöder, F., Kato, E., Sands, R. D., Sano, F., Tsutsui, J., Doelman, J., Muratori, M., . . . Yamamoto, H. (2022). Global biomass supply modeling for long-run management of the climate system. *Climatic Change*, *172*(1), 3. https://doi.org/10.1007/s10584-022-03336-9

Schaphoff, S., Forkel, M., Müller, C., Knauer, J., von Bloh, W., Gerten, D., Jägermeyr, J., Lucht, W., Rammig, A., Thonicke, K., & Waha, K. (2018). LPJmL4 – a dynamic global vegetation model with managed land – Part 2: Model evaluation. *Geoscientific Model Development*, *11*(4), 1377-1403. https://doi.org/10.5194/gmd-11-1377-2018

Schaphoff, S., von Bloh, W., Rammig, A., Thonicke, K., Biemans, H., Forkel, M., Gerten, D., Heinke, J., Jägermeyr, J., Knauer, J., Langerwisch, F., Lucht, W., Müller, C., Rolinski, S., & Waha, K. (2018). LPJmL4 – a dynamic global vegetation model with managed land – Part 1: Model description. *Geoscientific Model Development*, *11*(4), 1343-1375. https://doi.org/10.5194/gmd-11-1343-2018

Shen, Z., Hamelin, L., & Tiruta-Barna, L. (2023). Converting carbon vulnerable lands to wood plantations for use as building materials: Overall environmental performance and time-dependent assessment of carbon dioxide removals. *Journal of Cleaner Production*, *388*, 136040. https://doi.org/https://doi.org/10.1016/j.jclepro.2023.136040

Silver, W. L., Kueppers, L. M., Lugo, A. E., Ostertag, R., & Matzek, V. (2004). CARBON SEQUESTRATION AND PLANT COMMUNITY DYNAMICS FOLLOWING REFORESTATION OF TROPICAL PASTURE. *Ecological Applications*, *14*(4), 1115-1127. https://doi.org/https://doi.org/10.1890/03-5123

Smith, P., Nkem, J., Calvin, K., Campbell, D., Cherubini, F., Grassi, G., Korotkov, V., Hoang, A. L., Lwasa, S., McElwee, P., Nkonya, E., Saigusa, N., Soussana, J.-F., & Taboada, M. A. (2019). *Interlinkages Between Desertification, Land Degradation, Food Security and Greenhouse Gas Fluxes: Synergies, Trade-offs and Integrated Response Options. In: Climate Change and Land: an IPCC special report on climate change, desertification, land degradation, sustainable land management, food security, and greenhouse gas fluxes in terrestrial ecosystem [P.R. Shukla, J. Skea, E. Calvo Buendia, V. Masson-Delmotte, H.- O. Portner, D. C. Roberts, P. Zhai, R. Slade, S. Connors, R. van Diemen, M. Ferrat, E. Haughey, S. Luz, S. Neogi, M. Pathak, J. Petzold, J. Portugal Pereira, P. Vyas, E. Huntley, K. Kissick, M. Belkacemi, J. Malley, (eds.)]*.

Soergel, B., Kriegler, E., Weindl, I., Rauner, S., Dirnaichner, A., Ruhe, C., Hofmann, M., Bauer, N., Bertram, C., Bodirsky, B. L., Leimbach, M., Leininger, J., Levesque, A., Luderer, G., Pehl, M., Wingens, C., Baumstark, L., Beier, F., Dietrich, J. P., . . . Popp, A. (2021). A sustainable development pathway for climate action within the UN 2030 Agenda. *Nature Climate Change*, *11*(8), 656-664. https://doi.org/10.1038/s41558-021-01098-3

Sonntag, S., Pongratz, J., Reick, C. H., & Schmidt, H. (2016). Reforestation in a high-CO2 world—Higher mitigation potential than expected, lower adaptation potential than hoped for. *Geophysical Research Letters*, *43*(12), 6546-6553. https://doi.org/https://doi.org/10.1002/2016GL068824

Springmann, M., Godfray, H. C. J., Rayner, M., & Scarborough, P. (2016). Analysis and valuation of the health and climate change cobenefits of dietary change. *Proceedings of the National Academy of Sciences*, *113*(15), 4146-4151. https://doi.org/doi:10.1073/pnas.1523119113

Steffen, W., Richardson, K., Rockström, J., Cornell, S. E., Fetzer, I., Bennett, E. M., Biggs, R., Carpenter, S. R., de Vries, W., de Wit, C. A., Folke, C., Gerten, D., Heinke, J., Mace, G. M., Persson, L. M., Ramanathan, V., Reyers, B., & Sörlin, S. (2015). Planetary boundaries: Guiding human development on a changing planet. *Science*, *347*(6223). https://doi.org/10.1126/science.1259855

Stenzel, F., Braun, J., Breier, J., Erb, K. H., Gerten, D., Matej, S., Ostberg, S., Schaphoff, S., & Lucht, W. (2023). Two complementary metrics for global model-based assessment of terrestrial biosphere integrity: human colonization of the biosphere and risk of ecosystem destabilization [in preparation].

Stenzel, F., Greve, P., Lucht, W., Tramberend, S., Wada, Y., & Gerten, D. (2021). Irrigation of biomass plantations may globally increase water stress more than climate change. *Nature Communications*, *12*(1), 1512. https://doi.org/10.1038/s41467-021-21640-3

Sterling, S. M., Ducharne, A., & Polcher, J. (2013). The impact of global land-cover change on the terrestrial water cycle. *Nature Climate Change*, *3*(4), 385-390. https://doi.org/10.1038/nclimate1690

Trybula, E. M., Cibin, R., Burks, J. L., Chaubey, I., Brouder, S. M., & Volenec, J. J. (2015). Perennial rhizomatous grasses as bioenergy feedstock in SWAT: parameter development and model improvement. *GCB Bioenergy*, *7*(6), 1185-1202. https://doi.org/10.1111/gcbb.12210

UNEP-WCMC, UNEP, & IUCN. (2020). *Protected Planet Report 2020.*

Venter, O., Sanderson, E. W., Magrach, A., Allan, J. R., Beher, J., Jones, K. R., Possingham, H. P., Laurance, W. F., Wood, P., Fekete, B. M., Levy, M. A., & Watson, J. E. M. (2016). Global terrestrial Human Footprint maps for 1993 and 2009. *Scientific Data*, *3*(1), 160067. https://doi.org/10.1038/sdata.2016.67

von Bloh, W., Schaphoff, S., Müller, C., Rolinski, S., Waha, K., & Zaehle, S. (2018). Implementing the nitrogen cycle into the dynamic global vegetation, hydrology, and crop growth model LPJmL (version 5.0). *Geoscientific Model Development*, *11*(7), 2789-2812. https://doi.org/10.5194/gmd-11-2789-2018

Willett, W., Rockström, J., Loken, B., Springmann, M., Lang, T., Vermeulen, S., Garnett, T., Tilman, D., DeClerck, F., Wood, A., Jonell, M., Clark, M., Gordon, L. J., Fanzo, J., Hawkes, C., Zurayk, R., Rivera, J. A., De Vries, W., Majele Sibanda, L., . . . Murray, C. J. L. (2019). Food in the Anthropocene: the EAT Lancet Commission on healthy diets from sustainable food systems. *The Lancet*, *393*(10170), 447-492. https://doi.org/10.1016/S0140-6736(18)31788-4

Winkler, B., Mangold, A., von Cossel, M., Clifton-Brown, J., Pogrzeba, M., Lewandowski, I., Iqbal, Y., & Kiesel, A. (2020). Implementing miscanthus into farming systems: A review of agronomic practices, capital and labour demand. *Renewable and Sustainable Energy Reviews*, *132*, 110053. https://doi.org/https://doi.org/10.1016/j.rser.2020.110053